Towards an emerging understanding of non-locality phenomena and non-local transport

PAPER • OPEN ACCESS

Towards an emerging understanding of non-locality phenomena and non-local transport

To cite this article: K. Ida *et al* 2015 *Nucl. Fusion* **55** 013022

OPEN ACCESS
IOP Publishing | International Atomic Energy Agency Nuclear Fusion
Nucl. Fusion **55** (2015) 013022 (19pp) doi:10.1088/0029-5515/55/1/013022

Towards an emerging understanding of non-locality phenomena and non-local transport

K. Ida[1], Z. Shi[2], H.J. Sun[2,3], S. Inagaki[4], K. Kamiya[5], J.E. Rice[6], N. Tamura[1], P.H. Diamond[3], G. Dif-Pradalier[7], X.L. Zou[7], K. Itoh[1], S. Sugita[8], O.D. Gürcan[9], T. Estrada[10] , C. Hidalgo[10], T.S. Hahm[11], A. Field[12], X.T. Ding[2], Y. Sakamoto[5], S. Oldenbürger[13], M. Yoshinuma[1], T. Kobayashi[1], M. Jiang[2], S.H. Hahn[3,14], Y.M. Jeon[14], S.H. Hong[14], Y. Kosuga[4], J. Dong[2] and S.-I. Itoh[4]

[1] National Institute for Fusion Science, Toki, Gifu 509-5292, Japan
[2] Southwestern Institute of Physics, Chengdu, People's Republic of China
[3] WCI Center for Fusion Theory, National Fusion Research Institute, Daejeon, Korea
[4] Research Institute for Applied Mechanics, Kyushu Univ., Kasuga, Fukuoka, 816-8580, Japan
[5] Japan Atomic Energy Agency, Naka, Ibaraki-ken, 311-0193, Japan
[6] MIT Plasma Science and Fusion Center, Cambridge MA 02139, USA
[7] Association Euratom-CEA, CEA/IRFM, F-13108 Saint Paul-lez-Durance Cedex, France
[8] Chubu Univ., 1200 Matsumoto-cho, Kasugai, Aichi 487-8501, Japan
[9] LPP, Ecole Polytechnique, CNRS, 91128 Palaiseau, France
[10] Laboratorio Nacional de Fusion, Asociacion EURATOM-CIEMAT, 28040 Madrid, Spain
[11] Department of Nuclear Engineering, Seoul National University, Seoul, Korea
[12] Culham Centre for Fusion Energy, Abingdon, Oxfordshire, OX14 3DB, UK
[13] Itoh Research Center for Plasma Turbulence, Kyushu Univ., Kasuga, Fukuoka, 816-8580, Japan
[14] National Fusion Research Institute, Daejeon, Korea

Received 1 February 2014, revised 5 August 2014
Accepted for publication 19 September 2014
Published 5 January 2015

Abstract

In this paper, recent progress on experimental analysis and theoretical models for non-local transport (non-Fickian fluxes in real space) is reviewed. The non-locality in the heat and momentum transport observed in the plasma, the departures from linear flux-gradient proportionality, and externally triggered non-local transport phenomena are described in both L-mode and improved-mode plasmas. Ongoing evaluation of 'fast front' and 'intrinsically non-local' models, and their success in comparisons with experimental data, are discussed

Keywords: plasma, transport, non-local

(Some figures may appear in colour only in the online journal)

1. Introduction

One of the main goals in the study of turbulent transport in toroidal plasmas is to establish predictive capacity for the dynamics of burning plasmas. Indeed, considerable effort in the world magnetic fusion energy (MFE) research programme is devoted to the development and validation of simulation-based transport models, with the aim of prediction. For this purpose, formulae for transport fluxes (of heat, particle, momentum, etc.), i.e., the expression of fluxes in terms of plasma parameters and mean electromagnetic fields, have been pursued (see [1] and references therein). More precise knowledge has been obtained concerning the transport matrix, which describes the interaction between various gradients and fluxes (including, for example, the momentum flux, driven by the temperature gradient [2]). At the same time, experimental evidence has been accumulated regarding the breakdown of a 'local expression' of the flux-gradient relation (which ties the fluxes to gradients of mean parameters and gradients at the same location) in the Texas Experimental

Tokamak (TEXT), the Rijnhuizen tokamak project (RTP), and the Large Helical Device (LHD) [3–5]. One example of such non-locality phenomena is the spontaneous increase of core temperature associated with edge cooling by small impurity and hydrogen pellets which are observed both in tokamak and helical plasmas. This phenomenon manifests itself as a modification of the thermal diffusivity such that it decreases in the interior and simultaneously increases in the outer region [3]. The shell model is proposed as a physical explanation of why the thermal diffusivity interior region decreases [4]. In this model, the thermal diffusivity drops near the low order rational q surface, and therefore a slight change of q profile causes a large decrease of thermal diffusivity averaged over the rational surfaces interior region, where the magnetic shear is weak.

In contrast, the phenomena of spontaneous core temperature rise is also observed in helical plasmas, where the q profile is determined by magnetic fields produced by external coil currents and the q profile is unchanged after the edge cooling by pellets [5]. The observation of non-locality phenomena in LHD strongly suggests that the change in thermal diffusivity in the interior region is due to the change in temperature and the temperature gradient in the outer region, and not due to the change in the local magnetic shear. Simultaneous change of thermal diffusivity in both interior and outer regions are considered to be due to the strong coupling of turbulence in the two locations, separated by more than the scale length of micro-turbulence. This is called non-local transport. In general, it is difficult to discern distinguishing features of non-local transport in steady state, because any radial profile of temperature can be fitted within experimental error bars using ad hoc radially dependent thermal diffusivity profile.

Non-local transport manifests itself as 'non-local phenomena' only in the transient phase. Due to this modelling discrepancy, it is indeed possible that the contribution of the non-local transport is the dominant contribution in certain cases. The violation of the familiar local expression (local closure) compels us to explore new approaches to the predictive modelling for burning plasmas. Note that here we use the word 'local expression' in the sense that the relation is given in terms of mean parameters at the local position in space and at the same time. In particular, a successful transport model should be able to quantitatively predict *both* steady state *and* dynamical as perturbative transport phenomena. Therefore non-locality phenomena observed in various experiments constitute a set of novel and interesting *validation challenges* for prospective models of turbulent transport. Understanding of non-locality phenomena is central to the future development of theory and modelling of non-local transport.

In the study of plasma confinement, two simplifying assumptions have often been employed. (1) First, a local expression of the flux-gradient relation is expected to hold, because the fluxes are induced by microscopic fluctuations, the correlation length of which is much shorter than the gradient of mean parameters. (2) And second, if the local flux is induced by the local gradient, the response in transport would be diffusive. These viewpoints might be valid in some cases, but they have several serious limitations. The conjecture (1) must be updated, because there are many kinds of fluctuations with mesoscale correlation lengths. Considering the recent progress on the study of meso-scale and macro-scale fluctuations, such as zonal flows [6, 7], geodesic acoustic modes (GAMs) [8, 9], streamers [10–13], and global fluctuations [14, 15], or possible synergy between nonlinear spreading and toroidal couplings [16], it is natural that the local expression of flux-gradient relations is not set by local mean parameters. Energetic particles are another origin for global perturbations, and naturally introduce nonlocal effects in the energy balance dynamics (see, e.g., reviews [17, 18], and references therein).

The local closure of the flux-gradient relation (that is, to relate the local heat flux in terms of the local mean plasma parameters) can be violated even by microscopic fluctuations (the Eulerian correlation length of which is microscopic, e.g., ion gyro-radius). Turbulence spreading is predicted to appear in various circumstances where it can manifest itself in the form of ballistic spreading fronts [19–21]. This means that the conjecture (2) must also be re-examined. The local flux-gradient relation can indeed induce ballistic response due to nonlinearity, as is illustrated by an avalanche process related to the self-organized criticality models [22–25]. Temporally varying mean gradients in a 'stationary state' have also been reported, and the relation with the avalanche process was discussed [26]. The understanding of 'transient transport experiments' was assessed from these points of view [27]. Stimulated by these observations and studies of multiple-scale fluctuations, the research area of 'non-local' transport problems has developed rapidly. The objective of this article is to present a perspective for the present understanding of 'non-local transport' problems from the viewpoint of the violation of the local closure of the transport relation.

We first survey observations of the violation of 'local' flux-gradient relations, taking examples of recent studies such as the concave-convex transition [28, 29], tracer encapsulated solid pellet (TESPEL) injections, and supersonic molecular beam injection (SMBI) [30, 31]. Evidence for the non-local transport contribution is provided by dynamic response experiments, and the relative importance of this effect is discussed. Transport with these effects also expands our view of the realizable profiles, from the 'profile consistency [32]' or 'local stiffness picture [33, 34]' to 'selection of the global profile'. Here the 'local stiffness picture' is the concept that the heat flux is determined by the local temperature gradient and increases sharply when the gradient exceeds a critical value. This results in an apparent stiffness of the profile, so that the temperature profile does not change, regardless of the heating profile or strength.

In contrast, 'selection of the global profile' is the concept that the radial profile of temperature is not the result of an integrated temperature gradient determined by local transport, but is determined *globally*, by the strong and fast interaction between turbulence in the interior and outer regions of the plasma. Please note that this is a broader concept than the original rather narrow 'profile consistency' in ohmic plasmas, where the profile is determined by MHD activity sensitive to q-profile, not by the electrostatic turbulence. We next discuss the detailed study of fluctuations in conjunction with the non-local problem in transport processes. Long-range fluctuations (coherent and transient), and rapid and long-distance dynamics of microscopic fluctuations are explained. We then illustrate

theoretical progress. Theoretical considerations on the above-mentioned assumptions (1) and (2) are explained, and problem definitions for experimental identifications of essential processes are discussed. Thus, the efforts are accelerated to unite progress in experiment and theory. At the end, further challenging experimental observations are briefly explained. For clarity of argument, we stress the theme of 'violation of local closure' in this article. The motivation of this choice is to reduce ambiguities in the terminology of 'non-locality phenomena' or 'transient transport problem', which are often used in describing experimental observations. The new results and understanding reported in this paper are obtained from the discussion in the series of Asian-Pacific Transport Working Group meetings [35–37] and has been presented at the overview presentation at IAEA Fusion Energy Conference in San Diego in 2012.

2. Heat and momentum transport

In section 2, theoretical models and related experimental observations on the relation of heat and momentum radial flux to temperature and velocity gradients are summarized as an introduction. Let us take the radial heat flux driven by turbulence, $Q_{\mathrm{e,i}}(r)$, which is the sum of a convection flux and a conductive flux expressed as $T_{\mathrm{e,i}}(r)\langle\tilde{v}_r(r)\tilde{n}_{\mathrm{e}}(r)\rangle$ and $n(r)\langle\tilde{v}_r(r)\tilde{T}_{\mathrm{e,i}}(r)\rangle$, respectively. The conductive flux may be written using the local fluctuation intensity as $\langle\tilde{v}_r(r)\tilde{T}_{\mathrm{e,i}}(r)\rangle \propto -Re(\sum_{\vec{k}}|\tilde{\Phi}_{\vec{k}}|^2\tau_{c\vec{k}})\nabla T_{\mathrm{e,i}}(r)$ where $\vec{k}$ is the wave number of the turbulence and $\langle\rangle$ denotes the magnetic flux surface average. The central issue in the problem (whether the flux is expressed in terms of the local parameters or not) is thus formulated as whether the fluctuation intensities and the cross-phases are expressed in terms of the local parameters (at the same location and time) or not.

As a consequence of the mechanisms explained in the introduction, it has been considered that the relation between the flux and the gradient can be given by an integral form (in space and time). If one explicitly writes the spatial integral effect in a form using a kernel

$$Q(r) = -\int \kappa(r, r')\nabla T(r')\,\mathrm{d}r'. \tag{1}$$

A variety of approaches have been developed to model the kernel function analytical or simulation approaches [38, 39]. In the general case, the transport kernel structure may be characterized by a Levy distribution [38], which can be approximated as a Lorentzian of width Δ [39].

$$\kappa(r, r') = \Lambda/[(r - r')^2 + \Delta^2]. \tag{2}$$

The analyses related to the nonlocal kernel are explained in section 5. The key is to relate the shape of the kernel function to the width of the interaction Δ, and the strength Λ. It is also noteworthy that using an alternative kernel that is weakly non-local both in time and space leads to well-known flux-gradient relations such as Guyer-Krumhansl constitutive relations [40]. This approach actually provides the link between the Fisher-Kolmogorov equation approach discussed commonly in turbulence spreading and the strongly non-local formulations involving fractional diffusion.

As is stressed in the beginning of the introduction, recent developments of transport theory and simulation have demonstrated that (i) meso-scale and macro-scale fluctuations (which can violate local closure) exist, and that (ii) even microscopic fluctuations can induce mesoscale fronts and avalanches, which have a longer radial coherence length than the (Eulerian) correlation length of the consistent microscopic perturbations. If one quotes an example of dynamical equations for such microscopic turbulence and mean parameters (here, the temperature gradient is chosen as an example) from [21], the 'diffusion equation' for the temperature gradient and the evolution equation for the fluctuation intensity I (which is normalized to the kinetic energy density at diamagnetic drift velocity v_{dia}) are given by

$$\frac{\partial}{\partial t}A = D_0\frac{\partial^2}{\partial x^2}(IA) \tag{3}$$

and

$$\frac{\partial}{\partial t}I = \gamma_L(A)I - \gamma_{NL}I^2 + D_0\frac{\partial}{\partial x}I\frac{\partial}{\partial x}I, \tag{4}$$

where $A = \nabla T_a/T$ denotes the temperature gradient, $D_0 I$ is the 'diffusivity', γ and $\gamma_{NL}I$ are linear growth rate and nonlinear damping rate, respectively. One sees that this system of equations is fundamentally local, i.e., the right hand side (that induces temporal evolution) is described by the local values of parameters. Nevertheless, the one-to-one correspondence between fluctuation intensity and global plasma parameters does not hold, owing to propagating fronts. This is sometimes called weak nonlocality since the flux-gradient relation is no longer determined by a local algebraic relation, but instead as the solution of a set of partial differential equations, which physically propagate—possibly rapidly—the effect of gradient on the flux and vice versa. It is well known that the spatial positions of the peak of the mean plasma parameter (A in this case) and that of the fluctuation intensity (I in this case) are different. In this case, the one-to-one correspondence between gradient and flux does not hold.

The expression of mean (i.e., long-time average) global flux cannot be closed by mean global plasma parameters at the same position and time. That is, even if the instantaneous (but course-grained with respect to microscopic fluctuations) flux is explicitly given by a function of instantaneous local parameters (that includes avalanche-like modifications), super-diffusive propagation of the profile modification may possibly occur [26]. This invalidates any modelling approach, which relies on the Fick's law for the fluxes. Based on these theoretical results, it is now urgent to examine experimentally whether or not a local relation between gradient and flux holds. In particular, observations of fluctuations are essential to propelling the understanding: if a violation of local closure is found, the essential point is to identify what properties of fluctuations induce this violation.

Significant contributions of 'non-diffusive' term [41] have been recognized in the particle and momentum transport, while the 'non-diffusive' contribution is relatively small in the heat transport. Existence of 'non-diffusive' term causes the non-local transport to become more complicated, because both the diffusive and the non-diffusive term have non-local transport characteristics. The toroidal Reynolds stress $\langle\tilde{v_r}\tilde{v_\phi}\rangle$ is often written as $-\mu_\perp\nabla v_\phi + V_{\mathrm{pinch}}v_\phi + \Gamma_\phi^{RS}$ [42], the physics basis

Table 1. Experimental observations and theoretical models of non-local transport

Experiments	Phenomenology	Physics oriented observation	
Issue / Subjects pursued	'non-locality phenomena', that are not explained by diffusive process (and/or) Fick's law	violation of local closure, which relates the mean flux to the gradient of local mean parameters	
		Response in 'mean'	fluctuations
Core-edge coupling	Core temperature rise by Pellet, SMBI, LBO, modulated ECH	Hysteresis in g-f relation; 'potential' for selection of state	Long range fluctuations
Concave-convex ($\nabla^2 T$) transition	Concave-convex transition between two ITBs	Role of curvature; Enhanced transport across barrier	

Theory	Eq. for micro	Eq. for flux	Radial scale	Outcome
Meso and macro	Coupled with components with long radial coherence length	Given by micro (on each radius) and by meso-macro	coherence length of meso, macro; Front length	Nonlocal g-f relation
Avalanche	Not specified	Perturbed flux is related to perturbed T, on each radius	Length of avalanche	ballistic propagation, Super-diffusion
Fronts	With spreading, given on each radius	Given by micro, and closed on each radius	Length of front propagation	ballistic propagation, Super-diffusion

for which is fully explained in [43]. The first term is driven by the velocity gradient, while the second and third terms are independent of the velocity gradient, and are called 'non-diffusive' terms. The second term, which is proportional to the velocity itself, is called the pinch term and changes its sign depending on the direction of rotation (co- or counter-rotation). In contrast, the third term is called the residual stress term, which does not explicitly depend on velocity shear or on the velocity. Some models categorize it as an off-diagonal term of the transport matrix [44–46] but the contribution of radial propagation of waves to this term has also been pointed out [43, 47]. The radial propagation of waves and turbulent acceleration [48, 49] could be the origins of the violation of local closure, too. Considering the fact that the 'diffusion term' for heat flux is not always closed in a local form in terms of global parameters at the same position and same time, as is explained above, both the gradient-driven term as well as the residual term in the momentum flux can break the local closure. Keeping these in mind, we shall explain the experimental observations.

The survey of the issues in this section illustrates that the processes that are called *nonlocal* have various aspects and the adjunctive *nonlocal* has been used for various reasons. Thus, before going into the details of experimental observations and theoretical models, it might be useful to compare various approaches in a table, so that the reader can carry a map while surveying complicated behaviours of plasmas (which are not understood within the conventional picture that the transport flux is determined by the local plasma parameter). Table 1 explains various approaches to the emerging understanding of nonlocality in plasma transport. Experimental observations are on the one hand focused on the phenomenological observations, which try to describe in what manner the local closure (i.e., the effort to relate the flux to the local mean plasma parameters) is violated. At the same time, efforts are made to identify the cause and mechanisms that induce the violation of local closure. When the contribution to these two physically posed issues is not clear yet, one may use 'nonlocality' (with quotation marks). The phenomena, which are shown as examples, are the curvature transition, the fast core-temperature rise after edge-cooling, the flow-reversal phenomena, and the dynamics near L- to H-mode transition. Theoretical modellings are explained in later sections. Depending on the models, descriptions of the microscopic fluctuations are different, as is shown in table 1. The origin that causes long-range dynamics is also explained, and the outcome of the analysis is denoted. All of the avalanche models, front theories, and the theories which include the meso- and macro-scales fluctuations can explain some aspects of the violation of local closure. Each of these models focuses upon selective issues, so as to explain physics processes that are related to the nonlinear mechanisms in the models. They illuminate many essential elements, which might induce the violation of local closure, and are highlighted in the table.

There are kinds of touchstones, which are given by dynamical measurements. The first is the observation of the hysteresis in the flux-gradient relation, with the basis that the known gradients of mean plasma parameters cannot resolve the hysteresis in the local closure. The second is the long-rang fluctuations. The long-range fluctuations, being influenced by plasma parameters within their correlation length, interact with micro-turbulence that drives transport. Third is the radial propagation of change of intensities of microscopic turbulence. When such a dynamic exists, the local intensity of turbulence (thus turbulence-driven transport) at one location is influenced by dynamics at distance beyond the correlation length of micro-turbulence.

3. Violation of local closure in transport

3.1. Definition of non-local transport and hysteresis in the flux-gradient relation

The definition of non-local is that the local closure of transport relation (the radial flux is a function of the mean

plasma parameters and their gradients at the same position) is violated. In general, the momentum transport is non-diffusive because the momentum flux contains pinch term and residual stress term as well as diffusive term. However, this non-diffusive momentum transport is categorized to the local transport if these non-diffusive terms are determined by the local parameters such as flow velocity, temperature, and pressure gradient at the same position. Therefore, the transport phenomena can be classified as (1) diffusive and local, (2) diffusive and non-local, (3) non-diffusive and local and (4) non-diffusive and non-local. The core temperature rises associated with the edge cooling would be classified to (2) non-diffusive and local, while the flow reversal due to residual stress would be classified to (3) non-diffusive and local or (4) non-diffusive and non-local. In this article, the non-locality of the non-diffusive term will not be discussed, because there are no clear experimental results that show non-locality in the non-diffusive terms.

The non-locality (following our definition) often appears as multi-state of heat flux for a given temperature gradient or other gradients and the hysteresis relation between heat flux and temperature gradient in the transient phase. This multi-state discussed in this article is different from the multi-state in the transport between L-mode and improved modes where the local turbulence level and heat flux are affected by the local parameters such as radial electric field shear or magnetic shear. The hysteresis relation in the self-regulated oscillations or perturbed experiment (in which transport flux is not determined by the local plasma parameters and electric field) is considered to be a footprint of non-local transport. This is because the hysteresis relation is the result of the heat flux and turbulence level change before the local temperature gradient and local parameter (e.g. radial electric field shear or magnetic shear) at the same position change. It should be noted that the hysteresis relation between turbulence level and local gradient is a key issue, not the relation between heat flux turbulence level, because local closure between heat flux and turbulence level is not violated. Local heat flux should be determined by the local turbulence level and local gradient.

In the steady state, the core-edge coupling of the heat flux and turbulence is not identified in experiment, because any radial profile of temperature can be fitted using ad hoc radially dependent thermal diffusivity profile. When the local closure in transport is violated, the magnitude of heat flux and turbulence are not determined by the local parameters such as temperature gradient. If the non-local transport has significant contribution to the transport, the magnitude of heat flux and turbulence levels can have multiple values for a given temperature gradient within the transport time scale where the other local parameters such as density gradient, radial electric field shear, and magnetic shear are constant. Therefore a hysteresis in the local flux-gradient relation in a short time scale can be considered to be a footprint of the existence of a non-local transport contribution. In order to study the hysteresis in the local flux-gradient relation, external or internal perturbation to the plasma which break the steady-state flux-gradient relation are necessary.

Simultaneous measurements of temperature gradient, heat flux, and Micro-turbulence intensity during the modulation electron cyclotron heating (MECH) in LHD show that the

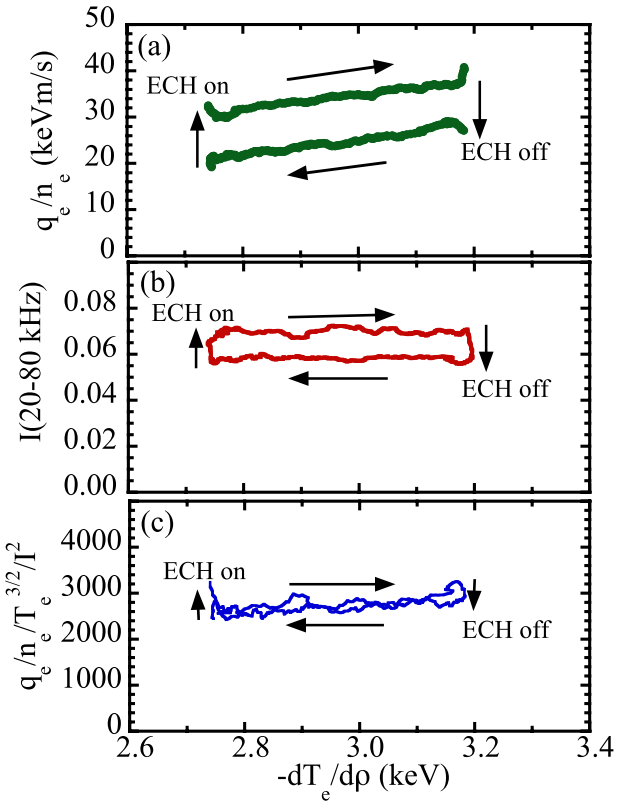

Figure 1. (*a*) Heat flux (*b*) intensity of fluctuation in the frequency range 20–80 kHz and (*c*) heat flux normalized by turbulence intensity as a function of temperature gradients during the modulated ECH.

temperature gradient responds to the heating power on the time scale of a few tens of milliseconds [50]. The difference in the time scales between responses in the gradients and the response in the heat flux to the ECH modulation clearly indicates that the heat flux and fluctuation intensity are not simple monotonic functions of the local temperature and local gradient. The changes in gradient and heat flux are drawn as a flux-gradient relation in figure 1. This result demonstrates a nonlinear relation (hysteresis) of the heat flux and fluctuation amplitude to the change in temperature gradient during the modulated ECH. This possible mechanism for this hysteresis is that the fluctuation amplitude and heat flux propagates radially from the core where the modulated ECH power deposits to the mid-radius of 2/3 of the plasma minor radius much faster than that of the increase of temperature gradient. The modulated ECH technique has been also applied in DIII-D in order to investigate the dynamic response of electron temperature and the heat transport. The difference in the time scales between responses in the gradients and the response in the heat flux to the ECH modulation clearly indicates that the heat flux and fluctuation intensity are not simple monotonic functions of the local temperature and local gradient. The changes in gradient and heat flux are drawn as a flux-gradient relation in figure 1. This result demonstrates a nonlinear relation (hysteresis) of the heat flux and fluctuation amplitude to the change in temperature gradient during the modulated ECH. This possible mechanism for this hysteresis is that the fluctuation amplitude and heat flux propagates radially from the core where the modulated ECH power deposits to the mid-radius of 2/3 of the plasma

minor radius much faster than that the increase of temperature gradient. The modulated ECH technique has been also applied in DIII-D in order to investigate the dynamic response of electron temperature and the heat transport. This is clear experimental evidence that the turbulence intensity and heat flux drive are directly influenced by the heating power in addition to the temperature gradient.

There are other various non-locality phenomena that show the hysteresis of flux-gradient relation and the violation of local closure of transport. In this paper, two non-locality phenomena are discussed below. One is spontaneous profile change (oscillation of the second derivative of temperature profile) in the ITB plasma for the constant heating power and the other is a transient temperature rise associated with the edge cooling caused by tracer encapsulated solid pellet (TESPEL) injection or supersonic molecular beam injection (SMBI). The former is called curvature transition and the latter is called non-local temperature rise. In both phenomena, a clear hysteresis of flux-gradient relation are observed in experiment.

3.2. Transition between concave and convex ITBs

The spontaneous transition between two transport states in plasmas with internal transport barriers (ITBs) is observed during the steady state phase (constant q-profile) in JT-60U [28]. These two states are distinguished by the change in sign of the second derivative of the ion temperature profiles (curvature); one has a concave shape (positive second derivative) and the other a convex shape (negative second derivative) without a change in temperature at the foot point and shoulder point of ITB. In the curvature transition between the concave and convex ITB, a simultaneous increase and decrease of the temperature gradient nearby takes place, which suggests that the turbulence intensity is not determined by the local gradient, but rather by the nearby gradient, inside the ITB region.

It is interesting that this non-local transport characteristic causes anti-correlation of temperature gradient nearby and sometimes triggers the oscillation phenomena between concave and convex ion temperature profiles as seen in figure 2(a). This oscillation may cause a severe collapse at $t = 5.69$ s by an MHD instability due to too large a pressure gradient. The spontaneous transition between concave and convex ITBs is a good example of the violation of local closure in the transport because (1) there are two metastable eigen-profiles of the ion temperature that are not determined by the local transport (flux-gradient relation) (2) and the change of transport cannot be explained by the change of local (or global) plasma parameters. It should be noted that the experimental evidence for the existence of an 'oscillation' between two states clearly shows that non-locality of heat transport can occur both in space and in time (as a memory effect). The temperature gradients at $\rho = 0.58$ and $\rho = 0.71$ at the end of concave state ($t = 5.55$ s) are close to those at the beginning of the concave state ($t = 5.41$ s), however, the behaviour afterwards is completely different, as seen in figure 2(a). This observation suggests that the transport is not solely determined by the present state of plasma parameters and implies that the transport during this curvature transition has a strong non-Markovian process feature. 'Non-local' transport plays an important role in this oscillation in temperature gradient and heat flux, and it causes the instability of heat transport, where the spontaneous rise and fall of the temperature gradient takes place even with constant heating power. Therefore, understanding the mechanism causing 'non-local' transport is essential to control the plasma and achieve good confinement. In fact, a minor collapse occurs at $t = 5.68$ s in this example, when the ion temperature gradient at $\rho = 0.58$ reaches $32\,\mathrm{keV\,m^{-1}}$. This suggests that ∇T_i oscillation (unstable transport) due to the 'non-local' transport triggers the MHD instability by exceeding the threshold for pressure gradients. In order to achieve a stable plasma with ITBs, the amplitude of the ∇T_i oscillation should be reduced, because even if the ∇T_i value transiently exceeds the critical value for the MHD stability during this oscillation, a minor collapse takes place and the good performance of the discharge with the ITB is terminated. The stability of transport is a very important issue because high transport stability will be required in burning plasma, where the fraction of external heating power becomes small.

In order to demonstrate that the local heat flux is not solely determined by the local mean plasma parameters, the flux-gradient relation during the oscillation is investigated and simultaneous opposite change in flux-gradient relation nearby is clearly observed. Figures 2(b) and (c) show the flux-gradient relation at two locations nearby $\rho = 0.53$ and $\rho = 0.67$ inside ITB region for the one cycle of the oscillations. The detailed radial profiles of ion temperature in an ITB plasma with concave shape and with convex shape are also plotted. Associated with the transition from concave shape ITB to convex shape ITB, the radial heat flux normalized by density drops transiently and the temperature gradient decreases at $\rho = 0.53$, while it increases at $\rho = 0.67$ even in the recovering phase of the radial heat flux to the original values. The flux-gradient relation observed during the transition phase is considered to be clear evidence of non-local transport, where the local heat flux is not determined by the local temperature gradient, but strongly affected by the temperature gradient nearby. The scale of the curvature transition region is $0.15(r/a)$, which is about 10 times the auto-correlation length of fluctuations [51]. The non-local contribution evaluated from the change in $\Delta(Q/n)$ during the curvature transition is 50% of the total heat flux as seen in figure 2(c). It should be also noted that the hysteresis direction is opposite between two locations nearby. The hysteresis direction is clockwise (CW) at $\rho = 0.53$, while it is counterclockwise (CCW) at $\rho = 0.67$. These observations are clear evidences that the local closure of heat transport is broken, because were the heat flux determined by the local gradient and other local quantities, the curvature of the temperature profile should be unchanged in steady state. If the turbulence intensity is determined locally, the transport can easily reach a steady state with a consistent temperature gradient, because the turbulence intensity increases as the gradient is increased, and larger turbulence intensity drives a reduction of the gradient for fixed heat flux.

3.3. Appearance of violation of local closure by perturbations

In general, the flux gradient relation in transport ($(Q/n) - (\nabla T)$) need not be determined by local parameters alone [1].

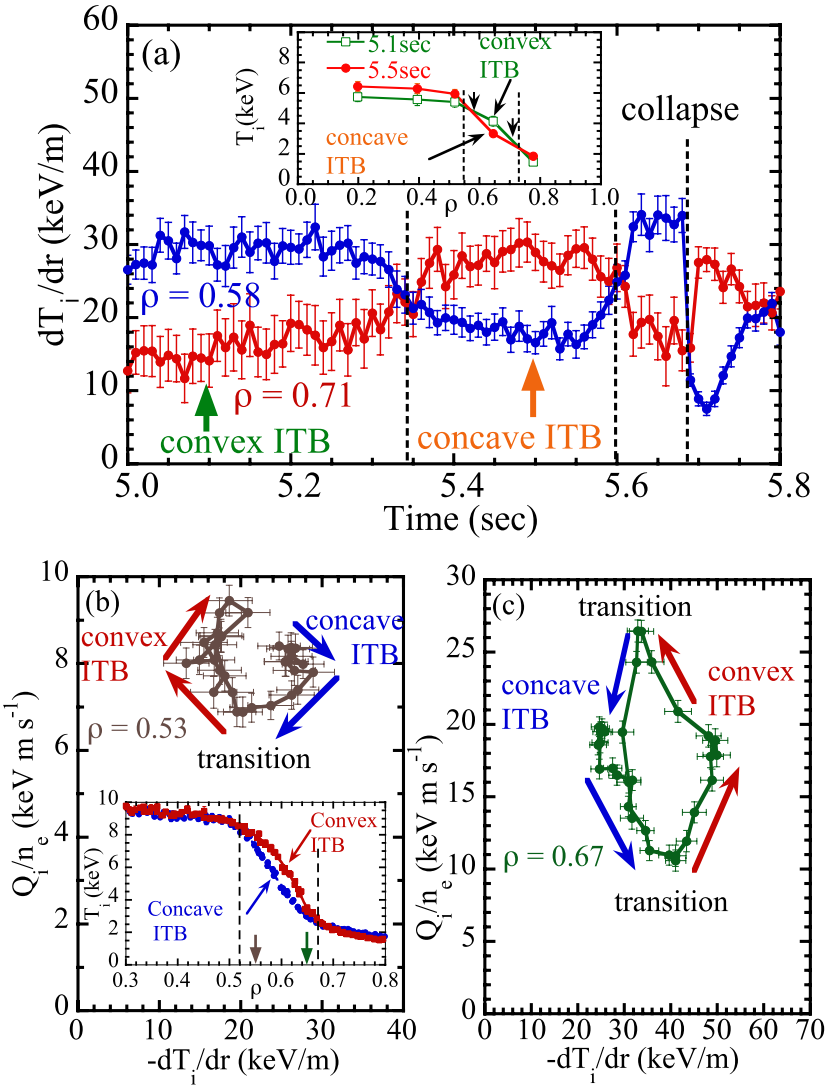

Figure 2. (*a*) Time evolution of ion temperature gradients at two locations inside the ITB region ($\rho = 0.58$ and $\rho = 0.71$), that are indicated with arrows in the radial profile in the ion temperature profile. Flux-gradient relation at two location nearby (*b*) $\rho = 0.53$ and (*c*) $\rho = 0.67$ inside ITB region during the transition phase from concave shape ITB to convex shape ITB in JT-60U. These two locations are indicated in the radial profiles of ion temperature in the concave and convex ITB plasmas.

However, the violation of local closure in transport is not clearly identified in steady-state plasmas, except during the period of transition phenomenon. This is because even if the 'non-local' contribution is as large as the others, the usually observed profile resilience (stiffness) introduces a collinearity between ∇T at different locations, so that the separation of the 'non-local' term from the others becomes difficult in steady state. Perturbation experiments provide a useful approach to test local closure of the transport, because a Lissajous figure of $\Delta(Q/n)$ plotted as $\Delta(\nabla T)$ shows how the local closure is broken. When there are two heat fluxes for a given local temperature gradient, the results suggests that the local and linear transport is not valid. Although the 'non-local' contribution may be evaluated from the hysteresis of $\Delta(Q/n)$ and is $10--30\%$ of the total heat flux, it causes a change in the temperature which is much faster than the diffusive processes.

Similar 'non-local' transport phenomena were observed in helical plasmas where there is no significant plasma current during experiments with tracer encapsulated solid pellet (TESPEL) [52, 53]. Figure 3 shows the time evolution of electron density (n_e), increment of electron temperature (δT_e), and electron temperature gradient ($\partial T_e/\partial r$) after TESPEL injection in LHD. The electron temperature decreases near the plasma periphery ($r/a > 0.6$), while an increase of electron temperature is observed in the core ($r/a < 0.5$), where the electron density is almost unchanged. Because of the simultaneous drop of the edge temperature and the rise of the core temperature, the temperature gradient increases transiently in the plasma. The time behaviour of the core temperature gradient is quite different from that of the edge temperature. The temperature gradient at $\rho = 0.67$ jumps to 5 keV m^{-1} from 4 keV m^{-1} immediately after the TESPEL injection and stays in the larger gradient state for 15 ms. Then the temperature gradient start to decrease and returns to the level before the TESPEL injection. This larger gradient state is considered to be a metastable state of transport. Figures 3(*c*) and (*d*) show the flux gradient relation between increment of heat flux normalized by electron density and temperature

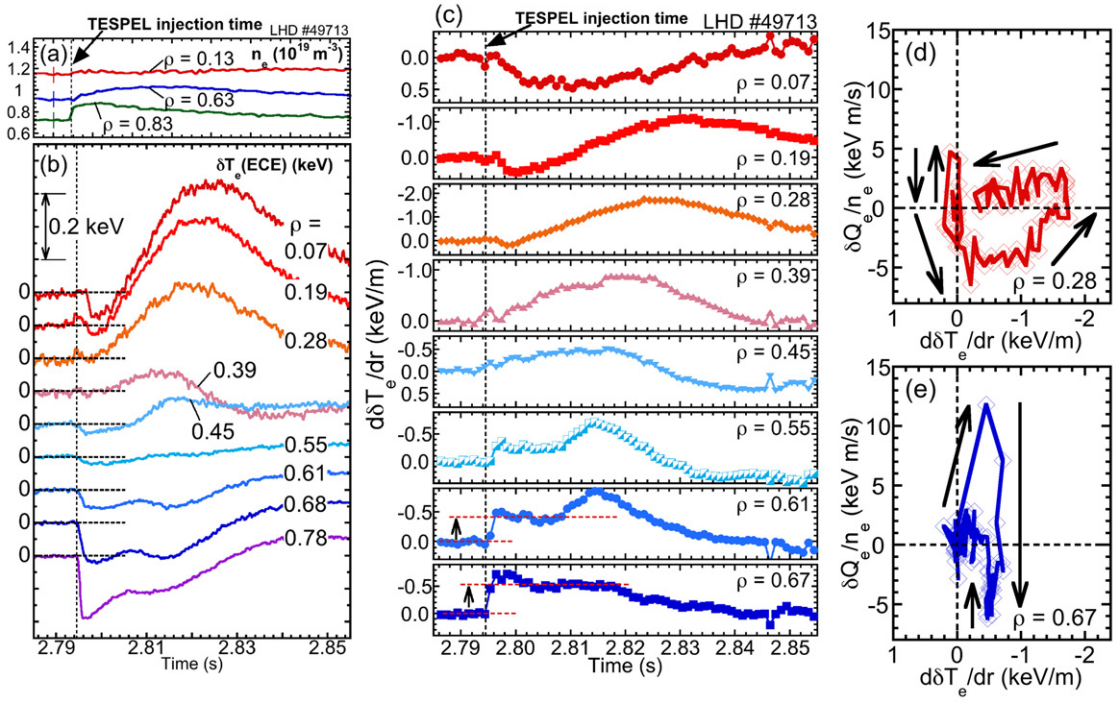

Figure 3. Time evolution of (*a*) electron density (n_e), (*b*) increment of electron temperature (δT_e), and (*c*) the electron temperature gradient ($\partial T_e/\partial r$) and flux-gradient relation at (*d*) $\rho = 0.28$ and (*e*) $\rho = 0.67$ after tracer encapsulated solid pellet (TESPEL) injection in the LHD.

gradient in the core at $\rho = 0.28$ and near the edge at $\rho = 0.67$. A clear hysteresis is observed in the core where the core temperature rise takes place. The direction of the hysteresis in the core is CCW, while it is CW near the edge. The reversal of hysteresis direction observed in this experiment is also one of the characteristics of non-local transport, which is similar to the discharge with curvature transition discussed above.

Recently, the PDF of $\Delta(\nabla T)$ during 'non-local' transport phenomena has been investigated in order to study the robustness of the transport flux landscape against deformations, and to evaluate the level of non-locality in the transport [54, 55]. A large deformation from the steady-state value ($\mathrm{d}\delta T_e/\mathrm{d}r = 0$) indicates that 'non-local' transport becomes dominant. The radial structure of the level of non-locality of transport has been experimentally determined by the contours of the PDF in the parameter space of (r/a, $\Delta(\nabla T)$) [56]. In order to investigate the dynamic response characteristics of the transport state, a deviation probability of the temperature gradient against the perturbation is evaluated with a transit time distribution (TTD) for a certain window $\delta(-\nabla T_e)$, which can be interpreted as an index of the extent to which plasma can be attracted by a certain transport state. Therefore, the TTD is considered to be a probability density function (PDF) of the displacement of the temperature gradients from the transport curve during the transient phase after the TESPEL injection. Figure 4(*a*) shows the TTD of the $\delta(-\nabla T_e)$ evaluated from the time evolution of temperature gradients plotted in figure 2(*b*). When there is only one transport state in the plasma, the probability density function, $P(\delta(-\nabla T_e))$, has one peak at zero displacement because the plasma stays around the transport curve. On the other hand, two peaks of the probability density function, $P(\delta(-\nabla T_e))$, appear when there are metastable states of transport in the plasma. The transport potential, S, can be determined from the probability density function, P as $P(-\delta\nabla T_e) = \exp(-S)$, which is a good parameter to indicate how the plasma responds to the perturbation and to the robustness of the transport [55]. When the transport is robust, the transport potential becomes deep because the plasma goes back to the original transport curve quickly after the perturbation. In contrast, the transport potential has two wells when there is a metastable state near the edge ($\rho = 0.67$) or a shallow profile when the robustness of the transport is weakened in the core ($\rho = 0.28$) during the transient phase, as seen in figures 4(*b*) and (*c*).

Figure 5 shows the time evolution of temperature and temperature gradient in a discharge with perturbation by supersonic molecular beam injection (SMBI) [30, 31] and density dependence of temperature rise after the SMBI. The core temperature increases, associated with the drop of the edge temperature after the each SMBI, although the heat flux in the core even decreases. It should be noted that the core temperature increase can be sustained over many energy confinement times by applying multiple SMBI in the discharge. This phenomenon is observed clearly in the early phase where the electron density is low, and tends to disappear as the electron density increases. It should be noted that the decrease of temperature rise is larger than $1/n_e$ and there is no temperature rise above the critical electron density of $0.8 \times 10^{19}\,\mathrm{m}^{-3}$, as seen in figure 5(*b*). The disappearance of temperature rise at higher density is also observed in the transition regime from liner ohmic confinement (LOC) to saturated ohmic confinement (SOC) in Alcator C-mod [60]. The disappearance of the core temperature rise after the edge cooling at higher density (collisionality) is a common phenomenon in toroidal plasmas.

The 'non-local' transport Äphenomena is also observed clearly in the ECH heated tokamak plasma at the event of the penetration of a large size carbon dust into the plasma in

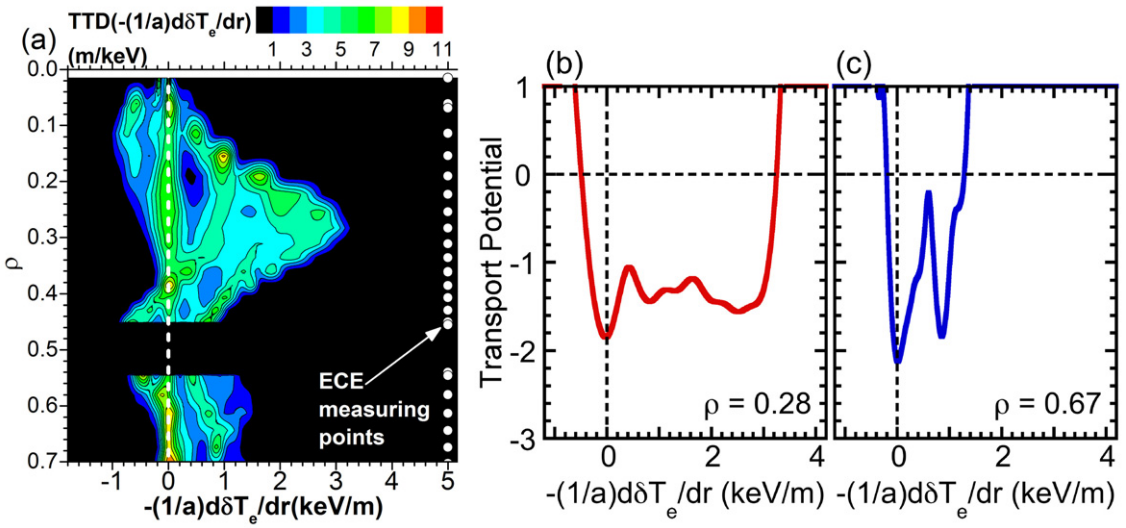

Figure 4. (*a*) Contour of the PDF in the space and temperature gradient, and transport potential, S, at (*b*) $\rho = 0.28$ and (*c*) $\rho = 0.67$ in the LHD evaluated from the data in figure 3.

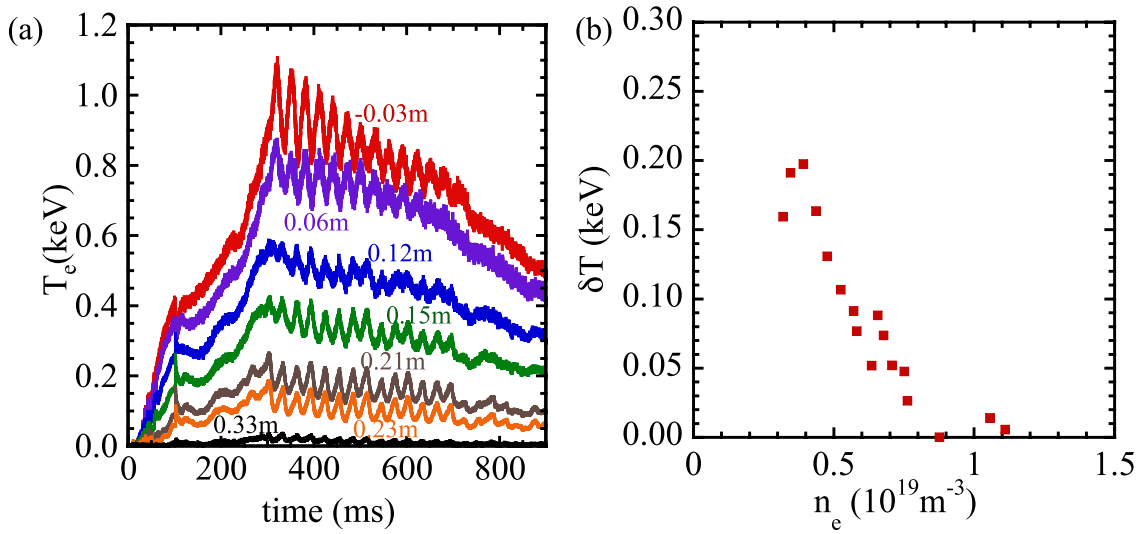

Figure 5. (*a*) Time evolution of electron temperature in a discharge with multiple SMBI and (*b*) increase of central electron temperature after the SMBI as a function of electron density in HL-2A.

KSTAR. The central electron temperature increases transiently ($\Delta t = 0.05$ s) associated with the cooling of the plasma edge by the dust. The increase of electron temperature (0.3–0.5 keV) is observed only in the region near the magnetic axis. The flipping of temperature rise/drop is located near the plasma centre ($\rho = 0.2$–0.3), which is in contrast to when the flipping location is in the middle of the plasma minor radius of $\rho = 0.5$ in HL-2A, LHD. The positions of flip depend on the edge safety factor of q_{95} in Alcator C-mod. The mechanism which determines the flipping location is not well understood and should be studied in the future. This experiment suggests the importance of plasma–dust interaction even in core transport not just in plasma edge–wall interaction.

3.4. Relation between energy and momentum flux

As we have noted earlier, the momentum transport is more complicated than heat transport due to non-diffusive effects and phenomena such as intrinsic rotation [42, 44, 57]. However since intrinsic rotation can be driven by temperature gradients [2, 58], there should also be a related non-locality of momentum transport in the plasma. Recent experimental observations of the bifurcation of intrinsic rotation magnitude [59] shows that the momentum flux at one location is not uniquely determined by local parameters at that location, and implies the existence of a direct non-locality of momentum transport. Non-locality of both heat and momentum transport can be investigated from the detailed analysis during a transient phase, such as the L/H transition, ITB formation, or the H/L back-transition.

Because the 'non-local' core temperature rise may be due to the change in the structure of turbulence in (k_θ, k_r) space, intrinsic rotation, which is due to the symmetry breaking of $k_\parallel$, should be correlated with 'non-local' transport. Recently the relation between the confinement regime (LOC and SOC), and the response of 'non-local' transport (core temperature

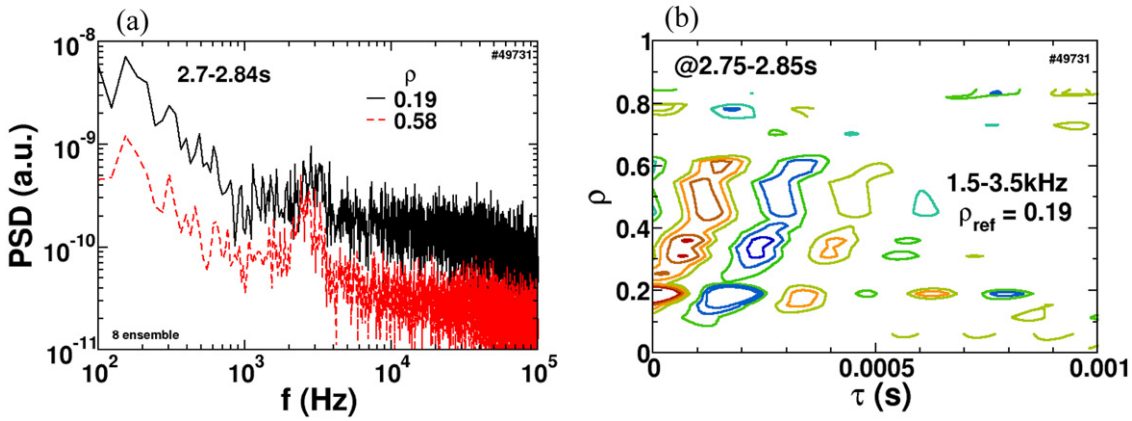

Figure 6. (*a*) Auto-power spectrum of $\tilde{T}_e$ at $\rho = 0.19$ and 0.58 (from [15] Reproduced with permission from Inagaki S. *et al* 2011 *Phys. Rev. Lett.* **107** 115001. Copyright 2011 by the American Physical Society.) and (*b*) Contour plot of the cross-correlation function of the low-frequency component (1.5–3.5 kHz) in the LHD.

rise or drop) and the direction of intrinsic rotation (co-rotation or counter-rotation) has been studied in Alcator C-Mod [60]. Rises in the electron temperature are observed only in the LOC regime (lower collisionality). At the higher electron density, the temperature rise (positive value) disappears and a temperature drop (negative values) is observed. The intrinsic rotation also changes sign from co-rotation (positive value) to counter-rotation (negative values). These observations clearly show that both the 'non-local' response (T_e rise or drop) and the sign of intrinsic rotation (co- or counter-rotation) are quite different between the confinement regimes (LOC and SOC), where the turbulence structure (turbulence mode) is different [47, 61, 62]. This experiment suggests a possible connection between the appearance/disappearance of 'non-local' response and the direction of intrinsic rotation in the co-/counter-direction. However, further study is required to investigate whether this connection observed is a coincidence or there is a causal relationship between the 'non-local' response and intrinsic rotation. It should be emphasized that 'non-local' phenomena and intrinsic rotation are not always observed together.

4. Fluctuations associated with 'non-local' response

4.1. Self-organized criticality

Associated with self-organized criticality, avalanche-like events in the energy transport are observed in the electron temperature fluctuations in DIII-D tokamak plasmas. The two-point cross-correlation function measured with ECE allows determination of a characteristic velocity. The effective velocity (the velocity of the peak of the cross correlation) is approximately constant at 10^2 m s^{-1} in the core and 10^3 m s^{-1} near the edge [26]. The effective velocity becomes negative (inward) near the magnetic aixis, which can be interpreted as resulting from the prevalence of negative avalanches (i.e., holes) [63]. The self-organized criticality (SOC) behaviour of the edge plasma transport has been studied using fluctuation data measured in the plasma edge and the scrape-off layer of the biasing experiment in TEXTOR. It is found that the local turbulence is well de-correlated by the $E \times B$ velocity shear [64]. Perturbative transport experiments have been performed at the stellarator TJ-II. The inward propagation of edge cooling pulses induced by the injection of nitrogen is ballistic and does not fit well in the framework of a diffusive transport model, even if an ad hoc pinch term is included. Simultaneous inward and outward propagation of heat pulses eliminates an explanation in terms of a pinch [65].

4.2. Long-range fluctuations

The experimental observations discussed above (curvature transition, strong correlation between core heat flux and the temperature gradient at half of the plasma minor radius, and existence of a metastable state after perturbations) strongly suggest there should be some 'agent' to couple the micro-scale turbulence at different radii separated by a distance greater than the scale length of the turbulence. Coupling between the micro-scale turbulence determining the transport and meso-scale fluctuations and/or zonal flows has been proposed as one of the candidates for the 'agent' [7, 14, 39]. The energy exchange between zonal flows and micro-scale turbulence or between micro-scale turbulence and meso-scale turbulence (high k and low k turbulence) has been found in experiments [6, 66]. Recently, coupling between micro- and meso-scale turbulence with long-range correlation [15, 67] has been observed experimentally, and this turbulence with long-range correlation can be another candidate for the 'agent' to explain 'non-local' transport. Turbulence with a long-range correlation is identified in the electron temperature measured with ECE. As seen in the auto-power spectrum of temperature fluctuations in figure 6, a clear peak is observed at 2.5 kHz, with a bandwidth of 1 kHz in LHD plasmas. This peak is mode significant at mid-radius of $\rho = 0.58$, while the peak becomes small near the plasma centre of $\rho = 0.19$. The auto-power spectrum at the higher frequency, above 8 kHz, is contaminated by the thermal noise of the ECE signal. Figure 6(*b*) shows the contour plot of the cross-correlation function of the low-frequency turbulence (1.5–3.5 kHz). The radial propagation of low-frequency turbulence is due to the phase propagation of a spiral turbulence structure. The spiral structures observed have a long-range correlation both in the poloidal ($m = 1$) and radial directions, which differ from zonal flows ($k_\theta = 0$, $m = 0$) and MHD modes (localized at fixed ρ).

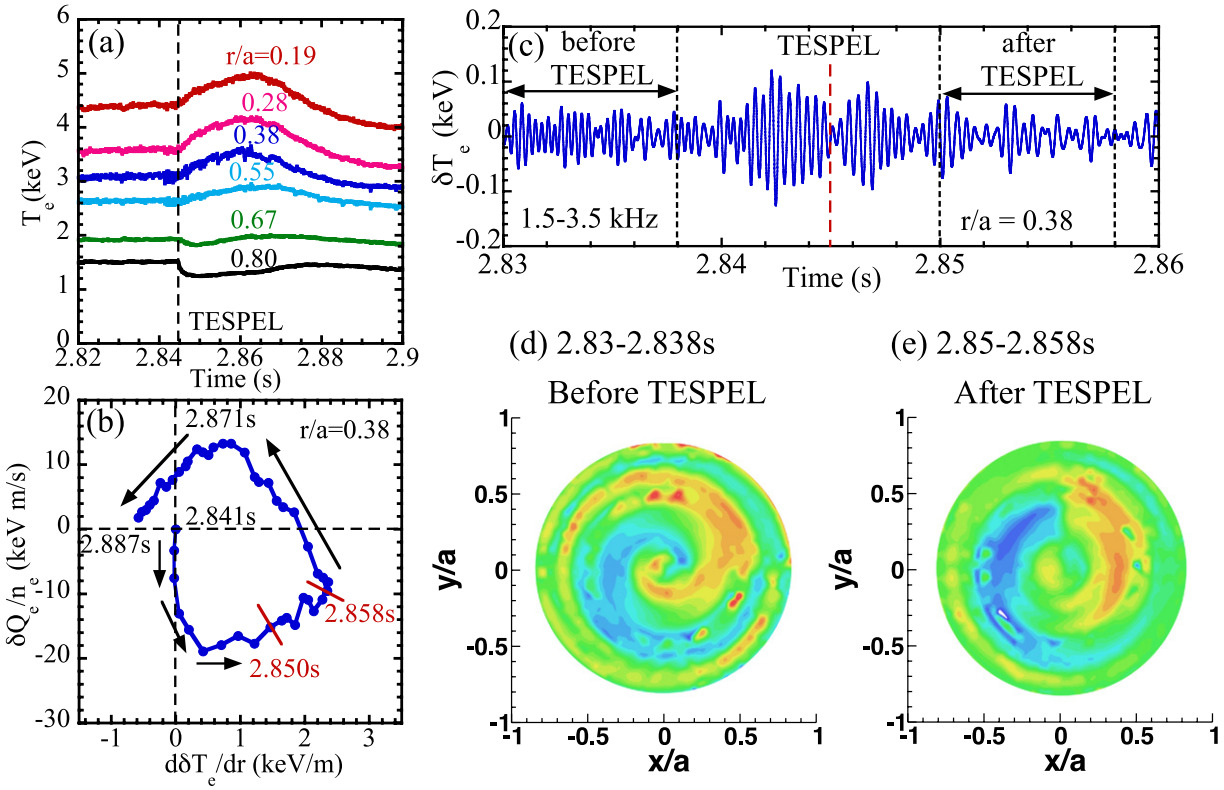

Figure 7. (*a*) Time evolution of electron temperature, (*b*) flux gradient relation between increment of heat flux normalized electron density and increment of temperature gradient at $r_{\rm eff}/a_{99} = 0.38$, (*c*) envelope of temperature fluctuation at low-frequency band (1.5–3.5 kHz) at $r_{\rm eff}/a_{99} = 0.38$ and reconstructed image plot of low-frequency turbulence structure on the poloidal cross-section, (*d*) before the TESPEL injection, and (*e*) after the TESPEL injection in LHD.

A possible candidate of this fluctuation has been discussed. Plasma parameters are in the banana regime for ions, $\omega_{\rm b,i} > \epsilon^{-1}\nu_{\rm i}$, ($\omega_{\rm b,i}$: bounce frequency of trapped ions, $\nu_{\rm i}$: ion collision frequency and $\epsilon = r/R$). For this observed perturbation, the phase velocity is larger than ion thermal velocity $v_{\rm th,i}$, and the frequency is higher than the ion bounce frequency. The relation $|k_\parallel v_{\rm th,i}| < \omega < \omega_{\rm b,i}$ is satisfied for the fluctuation of interest ($k_\parallel$: parallel wavenumber, and ω: angular frequency of wave). Thus, the observed fluctuation is conjectured to be linearly stable dissipative trapped-ion mode (DTIM). The dispersion relation was given for DTIM as $\omega_{\rm DTIM} = \sqrt{\epsilon/2}\omega_*$ and $\gamma = \epsilon^2\nu_{\rm e}^{-1}\omega_*^2/4 - \epsilon^{-1}\nu_{\rm i}$ [68]. Considering the positive mean electrostatic potential (which is of the order of $T_{\rm e}$), a Doppler shift of $\omega_{E\times B} \sim m \times 10^4\,{\rm s}^{-1}$ occurs (m: poloidal mode number). Thus, the dispersion relation in the laboratory frame for DTIM is $\omega_{\rm Lab} = \omega_{\rm DTIM} + \omega_{E\times B} \sim -(1+\sqrt{\epsilon/2})m \times 10^4\,{\rm s}^{-1}$. The observed frequency is close to $\omega_{\rm Lab}$, and the spectral width of excited fluctuations is close to damping rate $-\gamma$. Based on these analyses, DTIM has been proposed as a possible candidate. However, the DTIM is linearly stable. Therefore, a possible candidate of excitation of linearly stable DTIM is the coupling between this mode and microscopic drift wave turbulence [69]. Future studies will be conducted for the identification of the mode for understanding its excitation mechanism.

As is explained in table 1, theories have shown that the long-range fluctuations (the correlation length of which can be of the order of plasma radius) naturally cause the break down of the local closure of transport relations. The relation between the long-range fluctuations and breakdown of local closure has been discussed [70]. Although the electrostatic potential fluctuations play essential roles in the transport process, the heat flux is determined by the correlation between the temperature fluctuations and electric fluctuations. Therefore, the heat flux at the position of interest should be influenced by plasma parameters away from this point, if the temperature fluctuations have long radial correlation lengths (so that the temperature fluctuations at the position of interest are influenced by plasma parameters away from this point). The present experimental data of temperature fluctuations are relevant to show the breakdown of local closure of transport.

4.3. Fast changes of turbulence spectra

By assuming that the Doppler frequency of this mode is dominated by the $E \times B$ rigid rotation, the structure of this low frequency turbulence (1.5–3.5 kHz) can be reconstructed [71]. Figure 7 shows the time evolution of electron temperature, flux-gradient relation, envelope of temperature fluctuation at low-frequency band (1.5–3.5 kHz), and reconstructed image plot of low-frequency turbulence structure on the poloidal cross-section before and after the TESPEL injection in LHD. After the TESPEL injection at $t = 2.845$ s, the electron temperature in the core region of $\rho < 0.5$ starts to increase, while the temperature near the periphery drops due to injected impurity radiation. The flux gradient relation between the increment of heat flux normalized electron density and

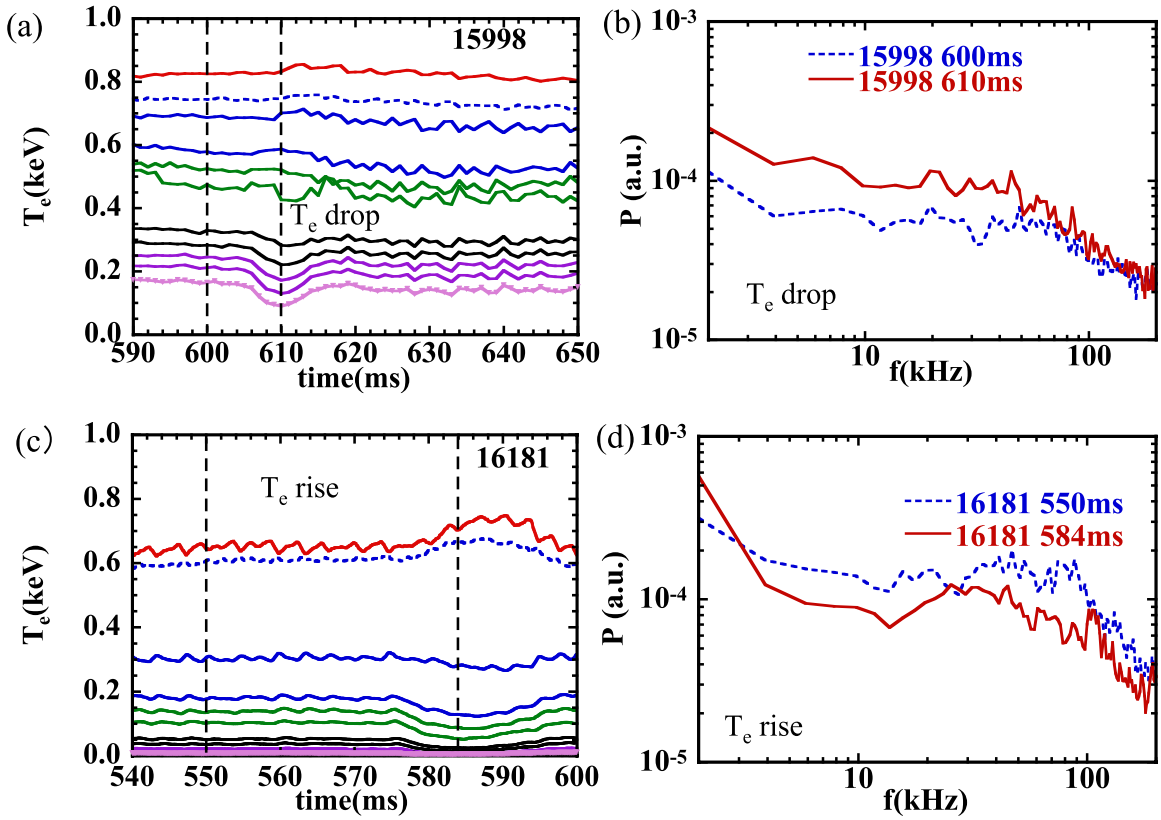

Figure 8. (*a*) Time evolution of electron temperature and (*b*) power spectra of fluctuations before ($t = 600$ ms) and after ($t = 610$ ms) the SMBI in the discharge without significant core temperature rise. (*c*) Time evolution of electron temperature and (*d*) power spectra of fluctuations before ($t = 550$ ms) and after ($t = 584$ ms) the SMBI in the discharge with significant core temperature rise in HL-2A.

increment of temperature gradient shows a clear hysteresis after the TESPEL injection in the time scale of ∼40 ms.

The envelope of temperature fluctuations at low-frequency band (1.5–3.5 kHz) shows the oscillations due to the $E \times B$ rigid rotation. The envelope starts to decrease after the TESPEL injection ($t = 2.845$ s) with a finite delay of 5 ms, as seen in figure 7(*c*). Before the TESPEL injection, the spiral structure extends from the plasma centre to the half-radius. After the TESPEL injection, the radial correlation of low-frequency turbulence becomes shorter, this spiral structure becomes less pronounced, and turbulence becomes more localized at the half radius. Turbulence with this spiral structure is a strong candidate for connecting the turbulence intensity at separated locations in the plasma. As seen in the contour plot of the cross-correlation function of the low-frequency component in figures 7(*d*) and (*e*), the radial correlation changes during the transient phase where the temperature gradient increases and hysteresis becomes maximum, as seen in figure 7(*b*), after the TESPEL injection [71]. Before the TESPEL injection, the radial correlation is quite long and turbulence at the plasma centre and at the half-radius are connected to each other. However, the radial correlation becomes shorter during the transient phase, after the TESPEL injection, which suggests the decoupling between the core and edge turbulence. Since the edge turbulence is larger than the core turbulence, the decoupling of the turbulence may contribute to the reduction of core turbulence, which would be one of the candidates of the mechanism to explain the core temperature increases. A working hypothesis, that the micro-turbulence intensity is modulated by this low k turbulence through modulational coupling, has been discussed [69]. This experiment clearly shows that during this transient phase, modifications occur in the phase relationship of this turbulence between the centre and half-radius and in the radial wavenumber of fluctuations, k_r.

Figure 8 shows the time evolution of electron temperature and power spectra of fluctuations before and after the SMBI in discharges without and with significant core temperature rise in HL-2A. In the discharge plotted in figure 8(*a*), there is no significant temperature rise associated with the SMBI, while the significant increase of temperature rise is observed in the discharge plotted in figure 8(*b*). Microwave reflectometry studies of the turbulent core density fluctuations show the dynamical response after SMBI. Initial observations suggest the alternation between small and large scale fluctuations. This requires further investigation of the role of multi-scale interactions in non-locality. Figure 8(*b*) shows the power spectra density turbulence measured with reflectometers (35 GHz) at $r/a = 0.9$ before ($t = 600$ ms) and after ($t = 610$ ms) the SMBI. The core electron temperature increases transiently after each SMBI associated with the drop of the edge temperature. The micro-scale turbulence (high frequency component of density fluctuations) is suppressed transiently and the meso-scale turbulence (low-frequency component of density fluctuations) shows a slight increase. If the edge-core coupling becomes strong due to the appearance of the meso-scale turbulence, this can lead to the suppression of core turbulence, which may explain the transient increase of core temperature. Turbulence measurement in the core, where

the temperature increases, is necessary to test this hypothesis in experiment.

It is more important to investigate how the structure of low k turbulence in (k_θ, k_r) space changes during the suppression phase. Although the radial cross-correlation function (CCF) of the meso-scale turbulence at $r/a = 0.9$ is almost unchanged during this phase, the poloidal CCF of the meso-scale turbulence shows a significant increase during the suppression phase of micro-scale turbulence ($t = 550$–584 ms). The maximum poloidal CCF increases from 0.1 to 0.2, while the maximum radial CCF increases from 0.13 to 0.18 after the SMBI pulse, as seen in figure 8(d). The clear increase of the poloidal CCF suggests the turbulent low-frequency structures are poloidally elongated during the suppression of micro-scale turbulence, which suggest that turbulent self-regulation via zonal-flows may be occurring. The relation between the poloidal elongation of the eddy and the $E \times B$ shear should be investigated in the future. Therefore, the core temperature rise triggered by the cold pulse is categorized by the transient formation of an internal transport barrier (ITB) based on the non-locality of transport. These experiments suggest that the nonlinear coupling between the turbulence in $(k_r, k_\theta, k_\parallel)$ space would be the most important issue in 'non-local' heat and non-diffusive momentum transport for an understanding of the "non-local" phenomena (curvature transition, core temperature rise) and intrinsic rotation in the plasma. The mechanism causing these phenomena (nonlinear coupling between the turbulence with different $\vec{k}$) always exists in the plasma and contributes to the dynamics of transport in $(t, r/a)$ space.

There are several possible mechanisms for the modulation of micro-scale turbulence. Zonal flows constitute one of the candidates to modulate the micro-scale turbulence in time and space (see review paper [7]). The energy exchange between zonal flows and drift wave turbulence which modulates the micro-scale turbulence level in time has been experimentally observed (see review paper [6, 72]). Moreover, the roles of the mean electric field and zonal flows at the L- to H-mode transition have been investigated both in experiment and theory [73–85]. It is a quite challenging experimental approach to measure the shape of the non-local kernel. The measurements of correlation between the turbulence magnitude and temperature gradient at the separate location would be a key issue, because the non-locality appears in the relation between the turbulence magnitude and temperature gradient not in the relation between the heat flux and turbulence magnitude [50]. The bi-coherence analysis of fluctuations at different radial locations due to a nonlinear coupling between micro-fluctuations and the long-range mode is also important approach to understand the physics mechanism in determining the shape of the kernel.

5. Relevant theoretical approaches

5.1. Introductory note

The theory of 'non-local' transport phenomena is still developing. In this section, we briefly survey theoretical approaches in the context of the phenomenology discussed in the preceding sections. This article classifies 'non-local' phenomena from the viewpoint of the violation of the local closure (in space and time) in the transport relation. This recognition of transport properties (violation of local closure) is assessed in the following way: (i) global transport properties in the formation of transport barriers, as an introduction for the universality of local closure violation, (ii) perturbation-induced 'anomalous response' in energy transport, (iii) generalization including momentum transport, and (iv) observations of multi-scale phenomena in fluctuations.

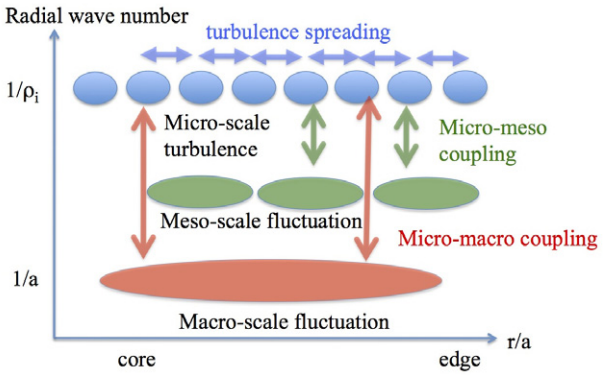

Figure 9. Illustration of elementary processes in multiple-scale turbulence.

Recent development in the theory of plasma turbulence has focused on the multiple-scale nonlinear and statistical dynamics of turbulence. Various processes are schematically shown in figure 9. A strong nonlinearity of the growth rate of the micro-scale turbulence can cause a ballistic front propagation of turbulence and gradient in radial direction, which is called avalanche. Then the turbulence and gradient can be radially coupled in the distance much larger than the turbulence correlation length. This has been known as turbulence spreading and can be a candidates for the non-locality phenomena, although the transport process itself is fundamentally local. Nonlinear coupling between the micro-scale turbulence and the meso- or macro-scale turbulence causes the interaction of turbulence and gradient in space, and is the most important process in the non-locality phenomena such as core temperature rise associated with edge cooling. The interaction between the micro-turbulence and zonal flow is categorized in the micro-meso coupling.

Rather clearly one can see a correspondence of these approaches to the experimental observations. The problems associated with front propagation are mainly explained in this article, because this is a prototypical example that local dynamics (i.e., weak non-locality) can induce a violation of local closure. It should be noted that the avalanche dynamics, which is in common with front propagation in the local diffusion model, can induce a violation of local closure and produce 'non-local' phenomena. The theory has been developed, but the experiments have not yet been fully studied. Then a few comments are made on topics in conjunction with macro- and meso-scale fluctuations and barrier formation problems.

5.2. Local mechanisms that induce 'non-local' responses

Avalanche, pulse, and front propagation models exploit the natural formulation of dynamical, 'anomalous response'

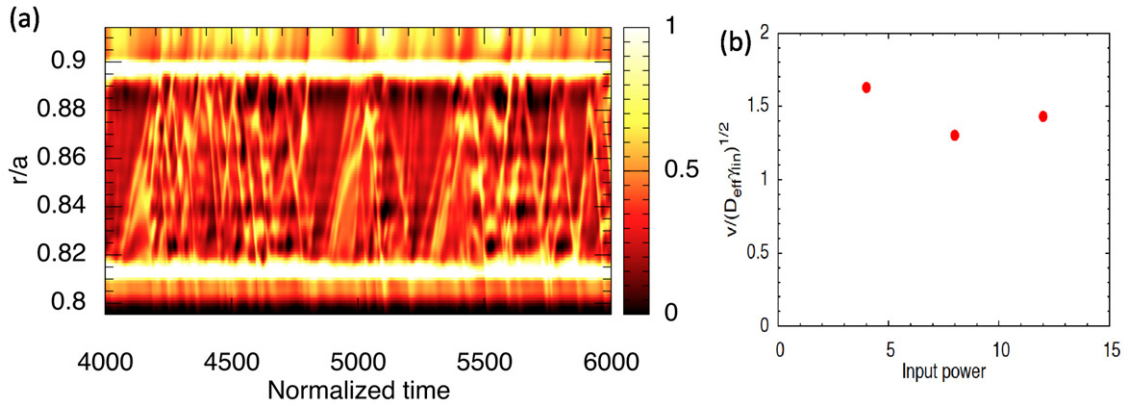

Figure 10. (*a*) Spatiotemporal turbulence intensity calculated with three dimensional edge turbulence simulation and (*b*) the ratio of Fisher front velocity in the turbulence simulation to the theoretical formula as a function of input power.

phenomena as a set of coupled, highly nonlinear reaction diffusion equations. Such systems have the property of exhibiting non-diffusive solutions in what naively appear to be diffusion equations. Classic examples of this are Fisher fronts, nonlinear diffusion–convection for turbulence spreading, and nonlinear wave packets. Studying this problem has two important illustrative examples in transport phenomena. First, this is a prototypical example to demonstrate why local closure of the flux-gradient relation is violated, although turbulent transport is usually expressed in terms of 'local fluctuations'. Second, though very simplified, studying this problem introduces a general guideline for the 'radial velocity' of super-diffusion propagation in response. The nonlinear damping process, which often arises from the cascade in wavenumber space (i.e., the transfer of energy via nonlinearity to highly stable components causes damping of the fluctuations of interest), causes the real-space diffusion of I. Due to this reason, $D_0 \frac{\partial}{\partial x} I \frac{\partial}{\partial x} I$ has similar properties to $\gamma_{NL} l^2$, where l is a characteristic spatial scale of fluctuations. (See [19, 20, 22, 118] for details.) Although equation (4) is given in terms of the 'local' equation, i.e., all terms are given by local parameters, solutions of such systems represent the ballistic (non-diffusive) response. Pulses have been shown to propagate at constant speed (Fisher front velocity), $v_r \sim \sqrt{\gamma D_0}$, where γ is the linear growth rate, which gives an order-of-magnitude estimate as $v_r \sim v_{\rm dia}$ for drift wave turbulence [20].

This is a prototypical example to understand 'super-diffusive response' in diffusive systems. The basic formulation of this class of models is fundamentally local but highly nonlinear. One can find a variety of work in this direction of thought. Recent simulations have shown that the relation of $v_r \sim \sqrt{\gamma D_0}$ gives a good approximation for a statistical average of a large number of excited pulses and fronts as seen in figure 10. (The detailed description of the simulation is given in [86].) The radial correlation length of these ballistic pulses was also studied, and the Lagrangian correlation length is a few times longer than the local correlation length [87]. The convergence to the long-time average has also been studied in detail by use of the Hasegawa–Wakatani model [88]. The deviation from the long-time average converges following the scaling law $1/\sqrt{N}$, where N is the number of events. The events last a significant fraction of the confinement time. The typical event duration is thus in the range of 5 correlation times, a ratio also reported in gyrokinetic flux driven simulations [39]. It is emphasized that the key aspect being that it is a local model for a second moment (i.e., the turbulent intensity) instead of a first moment (the profiles). Thus, the model that includes the fronts can illustrate the breakdown of local closure of transport relations in terms of mean plasma parameters. Indeed, the spatial positions of the peak of the mean plasma parameter and that of the fluctuation intensity (so of the flux) are different. The one-to-one correspondence between gradient and flux does not hold in the fronts. This process is now observable in experiments, and opportunities of new research have been given to experimentalists. The experimental reports on this are explained later.

Momentum transport has the property that it is sensitive to stresses, which are not simply proportional to velocity or its shear. These contributions, called 'residual stress' convert radial inhomogeneity into intrinsic torque density and flow drive by symmetry breaking. Developments in this issue are discussed in depth in the overview [43], where aspects of avalanche dynamics as well as long-range correlations are illuminated, and readers are referred to [43] for detailed arguments. An example of this process is taken from the cases of the co-intrinsic torque exerted by the edge transport barrier (ETB) in H-mode, due to Reynolds stress $\langle \tilde{v}_r \tilde{v}_\parallel \rangle$. An interesting property of residual stress is that it may be viewed as an effective, heat flux-driven internal source in the momentum balance. No counterpart in heat transport for such internal sources has been pointed out. Nevertheless, it is worth pointing out that the anomalous coupling/transfer between different plasma species has such properties (i.e., if one looks at the electron energy balance, a turbulence-driven source/sink appears), though it is not the divergence of a flux [89]. The nonlocal nature in the interaction between different species has also been discussed [89]. Thus, for example, counter-NBI deposited on axis in H-mode plasmas must work against the intrinsic co-torque in the pedestal. In one experiment, these two effects cancelled, leaving a state of zero rotation [90]. Such internal sources, say at the edge, thus have been shown to affect profoundly the momentum transport in the core, giving the flavour of a 'tail wags the dog' effect. Interestingly, here apparently 'non-local' phenomena emerge from a fundamentally local (through non-diffusive) model. The key aspect being that it is a local model for a second

moment (i.e., the turbulent intensity) instead of a first moment (the profiles).

The dynamics which are related with the fronts and avalanches have been shown in flux-driven simulations. Flux-driven fluid [23, 25, 91, 92] and gyrokinetic [93–95] systems are now in common use and have increasingly been reporting deviations from the local and diffusive paradigm, either confirming the ideas of avalanching and spreading or the characterization of non-local, non-diffusive behaviour [16, 19, 20, 22, 27, 39, 88, 96–100]. Since in flux-driven systems the only constraint is to ensure a balance, on average only, between the sources and the sinks, computations have shown that probability distribution functions (PDFs) of the particle flux [88] or of the heat and momentum flux [101, 102] display heavy tails towards the large positive values, that the effective flux is essentially sustained by the heavy tail part of the PDF. This property is typical of avalanche-like behaviour [22, 91–94, 103–105] and 1/f frequency spectra [22, 94, 103, 106, 107] are observed. Flux-driven gyrokinetics confirm this result as avalanche-like heat propagation has been shown to be still significant even though the mean field scaling are considered to be close to the familiar gyro-Bohm scaling [39, 108–110]. This observation indicates that the dimensional similarity of the mean heat flux to the gyro-Bohm scaling does not necessarily mean that the mean heat flux (at any radius) is given in terms of the local mean plasma parameters (at the same radius).

It is also a strong indication that an accurate modelling of the transport processes up to the confinement time seems crucial to characterizing the transport processes. Indeed, tracing the large flux events and determining their dynamics, there are indications that these events behave like fronts or avalanches such that the microscopic transport is close to ballistic [22, 39, 88, 107, 111], in marked difference with that assumed when considering the Brownian motion-based local paradigm. The fine details of the profile dynamics thus seem important for explaining these results. There is indeed mounting evidence which shows the importance of non-local interactions in plasma profile evolution which is related to meso-scale structure formation, should it occur through zonal flow pattern formation [39] or through fluctuations of the intensity envelope [112, 113]. Both approaches are different sides of the same coin as the intensity profile is related to spatial structure of the Reynolds stress, which is manifested through avalanching and pattern formation in the meso-scale range.

5.3. Additional issues including non-local fluctuations and their impact

When the meso-scale and macro-scale fluctuations are excited, the transport which is caused by these fluctuations is non-local [16, 27, 39]. Thus, if the transport relation is closed in terms of global plasma parameters and their gradients, the local flux-gradient relation is replaced by a non-local, integral relation in space, and possibly in time. The kernel of the integral may have a divergent second moment, indicative of a Levy process. The amplitude of the zonal flows is controlled by the integral of drive by microscopic fluctuations. Therefore, the back-interaction by zonal flows on the microscopic turbulence is not specified by local parameters, but influenced by fluctuations at

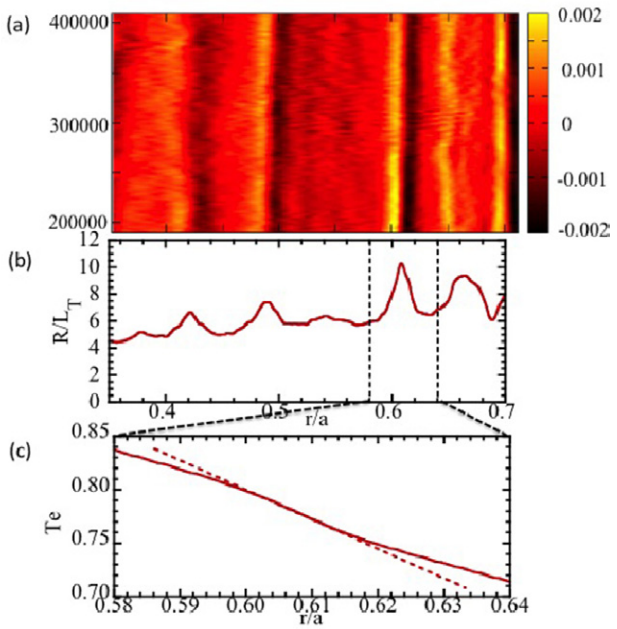

Figure 11. (*a*) Contour of radial electric field shear and radial profile of (*b*) temperature gradient R/L_T, where R is major radius and L_T is scale length of temperature and (*c*) calculated electron temperature, which shows multiple-scale dynamics and formation of a 'staircase' in the gradient.

a mesoscopically distant location, though within the coherence length of zonal flows. Thus, a non-local interaction like the 'seesaw mechanism' can work [114]. When the fluctuations are excited more strongly at one place, they can enhance the zonal flow, as well. The microscopic fluctuation at the other place can be reduced by the enhanced zonal flows. There is another process by which the meso-scale interaction can induce an intermittency of gradients. This coupling between small-scale turbulence and larger scales is done via meso-scale (mean) $E \times B$ flow shear, which is seen through the spontaneous generation of meso-scale patterns of $E \times B$ flows called an $E \times B$ 'staircase', as seen in figure 11 [39].

An $E \times B$ staircase is a quasi-periodic sequence of thin $E \times B$ shear layers and related profile corrugations, interleaved by regions of strong avalanche activity. In studying the staircase, the mean gradient is considered to be not smooth in radius, contrary to the conventional picture. Corrugations of mean gradient are induced by the nonlinear interaction between the turbulence and turbulence-driven $E \times B$ flow. When the gradient is not a smooth function in radius, but has peaks, the spatial profile of mean parameter takes a form like staircase. The $E \times B$ staircase is the plasma analogy to the potential vorticity staircase well known and often observed in geophysical fluids [115]. Both the potential vorticity and $E \times B$ staircases are formed by (effective potential vorticity) mixing processes with a finite mixing scale. The interstep spacing of the staircase constitutes an emergent scale similar to the Rhines scale [116] familiar from geophysical fluids dynamics, which denotes the largest scale of structure that the cascade of turbulence can produce on the rotating sphere. The $E \times B$ staircase is remarkable in that it resolves the natural competition between flow shearing and avalanching by separating these into distinct spatial domains. $E \times B$ staircases

are emergent phenomena, and are *not* a trivial consequence of imprinting by the magnetic geometry. In particular the locations of the 'step' in the core discussed in [39] are not correlated with low-q resonances. A particularly remarkable aspect of the $E \times B$ staircase is its quasi-periodic regularity amidst a background of stochastic avalanches. The discussion as to how these structures emerge is still ongoing, yet it has already been shown that the existence of these structures has some interesting consequences on shear, poloidal rotation and turbulent transport.

The mean $E \times B$ flows are driven by the mean pressure gradient, turbulence and other mechanisms [14, 117, 118]. It may compete against zonal flow [78]. The staircase is a long-lived pattern of shear layers; in simulations where such structures exist the mean shear is reported to be dominant as compared to the zonal flows shear [103]. From a modelling perspective, mean flows are associated with meso-scale structures on the mean profiles; A systematic procedure has shown that equations (1) and (2) are good fits to the turbulent heat flux Q. The size Δ of this kernel also coincides with both the typical step of the staircase and the typical avalanche size in the system. In-between the staircase steps, the transport is avalanche-dominated. How the stochastic avalanches may produce this quasi-regular flow pattern is under investigation. An analytic perspective is proposed by developing an analogy with the formation of traffic Jams [119]. For traffic jams, the finite delay time in the response of drivers plays the key role, while in the avalanche dynamics, the finite delay time in the response of turbulence intensity is essential.

These studies in sections 5.2 and 5.3 give a basis to an inductive approach, in which the integral relation like equation (3) (in terms of the space- (and time) integral) with a test kernel [96–100, 120, 121] has been inductively obtained by fitting to the experimental observations. This approach has stimulated the importance of the study of violation of local closure. Balescu has stressed that the continuous time random walk (CTRW) model might be more relevant than the diffusion model in which the time between consecutive jumps is considered to be a random variable, while the discrete time is used in usual random walk [122]. A mathematical framework for the fractional kinetics which is constructed on the fractional derivative has been developed [123]. This line of inductive approach is complementary to the picture of multiple-scale turbulence, and might be unified in the future. The influence of higher-order derivative terms on the flux [66, 124–128] is also related to nonlocal closure. When the effect of curvature is as important as that of the gradient, the effects of much higher order derivatives should also be considered: that is, the study must be expanded to include the integral formulation of transport fluxes.

6. Summary and discussion

In this article, we have explained the recent development of the research on plasma transport in magnetic confinement device, putting an emphasis on the issue of the violation of local closure of transport relations. That is, the new results in experiments as well as the new analyses of previously published experimental data are presented. Theoretical progress is also addressed in order to provide a few fundamental concepts that provide common views for varieties of experimental observations. By using the dynamical method to study the transport properties, we have shown that there are many observations, which clearly indicate the violation of local closure of transport relations. The position of this article is to present a view of the violation of local closure, in order to provide an organized approach for the long-lasting problems, which have been discussed under the terminology of transient transport problems or nonlocal transport problem. The advantage of this approach is proved in this article, by applying the new analysis method (e.g., the search of gradient-flux relation out of dynamical response of plasmas) to previously published data. This view of the breakdown of the local closure of transport relations, combined with this dynamical method in experiment will be powerful to organize many and complex phenomena in dynamics of plasma transport.

The experimental study for the mechanism of violation of local closure will be an interesting topic for future work. In concluding this article, some possible major impacts of this issue on future research are discussed. One is the identification of the mechanisms that introduce the (already observed) violation of local closure. The other is that the validation of the direct simulation codes and transport models should include comparisons with studies of dynamical responses, in addition to those with stationary states. This is a crucial element of future studies of non locality phenomena. In identifying the physical mechanisms, two have been emphasized; one is the fast front propagation of micro-scale turbulence, and the other is the coupling between micro-scale and meso/macro-scale turbulence. Measurements of spatiotemporal micro-scale turbulence in experiment are essential to test these models. The former process appears as an incoherent propagation of micro-scale turbulence, for which new experimental observations are emerging. For instance, D-III D has reported possible avalanches in the core plasma [26]. In addition, spatio-temporal dynamics of turbulence and gradient in the limit cycle oscillation near the edge plasma of JFT-2M are compared to front propagation dynamics [129–132]. As is noted in section 5, these two (the front propagation of micro-scale turbulence and the coupling between micro-scale and meso/macro-scale turbulence) approaches can coexist and cooperate. The Reynolds stress, which is manifested through avalanching and pattern formation in the meso-scale range, can generate the flows and fluctuations in meso-mean scales. The generated flows/fluctuations regulate the microscopic fluctuations.

In LHD, the intensity of micro-scale turbulence is found to be modulated by the frequency of long-range fluctuations ($\sim$2.5 kHz) and the transport driven by microscopic turbulence is modified by the appearance of long-range fluctuations due to the energy transfer between the microscopic turbulence and the long-range fluctuations. The reduction of high-frequency fluctuations occurs in conjunction with the long-range fluctuations [69], while the long-range fluctuation (note that $n \neq 0$ and $m \neq 0$ that differ from the zonal flow) itself induces additional transport. Comparing these two competing processes, the net transport is reduced by the appearance of these long-range fluctuations near the threshold condition of instability. More recently, the direct influence of central heating on turbulent transport at two-thirds of the

plasma minor radius has been identified in the LHD [50]. Related observations have been reported [133, 134]. The hysteresis appears in the gradient-flux relation, as well as in the relation between gradient and fluctuation intensity. This issue must be studied in much wider circumstances. This phenomenon can be understood with the conjecture that the modulation of heating power at the centre immediately influences the long-range fluctuations which modulate higher frequency fluctuations at a distance (correlation length of long-range fluctuations) through their nonlinear couplings [135, 136].

The rapid progress in the experimental measurement of the dynamics of turbulence will soon provide more quantitative information on the cause of violation of local closure for transport relations. It is a major challenge in experiments to measure the shape of the non-local kernel, because it would be a more definitive test of non-local transport models based on the different physics mechanisms. The scale length of the non-local kernel for the coupling of micro- and macro-turbulence is an auto-correlation length of the microscopic mode. On the other hand, the coupling length owing to spreading was pointed out to be few times of correlation length of microscopic turbulence [40, 137]. The former can be longer than the latter (few times the microscopic length), so that the non-local kernel for the coupling of micro- and macro-turbulence can have a much longer tail than that for turbulence spreading. It is also an interesting test how the non-local transport changes with MHD modes driven by energetic particles, because they can be also additional origins of global perturbations,

In the experimental observations, it may also be useful to note recent results of theory and simulations, in addition to fundamental elements explained in section 5. Turbulence spreading can also contribute to the mesoscale dynamics via the formation of heat waves [119, 137]. The fluctuating part of the temperature may indeed follow a wave-like equation to which a radial propagation speed is associated, which is in the ballpark of the observed radial propagation speed of the turbulence. Turbulence spreading might be mediated by GAMs [138] as GAMs have a radial group velocity [139] and are amplified in the edge via the beach effect [137]. In these respects, recent flux-driven gyrokinetic simulations of energetic GAMs (EGAMs) [140] have been performed in the presence of turbulence, which show that the presence of EGAMs is found to impact the mean temperature profile, therefore impacting the turbulence through a possible coupling between EGAMs and mean $E \times B$ flows [141]. The excitation of GAMs by energetic particles and the energy channelling to bulk ions [142] has been observed by experiments [143]. Thus, coupling of transport processes in wider circumstances, including velocity space non-locality (e.g., [144]), will be studied in the future.

The findings of non-local transport in experiments has a strong impact on the local transport model and simulation based on the turbulence determined by the local quantity. Comparison of simulation results with the experiments have been done with steady state profiles, not dynamically in the transient phase. Reproducing non-locality phenomena observed in experiment, where the transport and profiles at separated locations are correlated with each other, is a big challenge for simulation, because this is the definite test of the validity of the transport model. The comparison in the steady state profiles between experiments and simulation is not enough, because the non-local transport features can be identified only in the dynamics of transport, not in the steady state transport. In fact, there is no simulation which can reproduce the ITB radial propagation in the steady state configuration (for example, q-profile) observed in experiments [145, 146]. A preliminary report on the global nonlinear simulation has been made, and has examined the dynamical response against the periodic modulation of heating, where the violation of the local closure was demonstrated [147]. The dynamic transport simulation which can reproduce the non-local dynamics in experiments is desirable to understand non-local transport.

The importance of non-locality phenomena to the critical task of transport model validation *cannot* be over-emphasized. The escalating costs of ITER and DEMO drive us to demand a predictive model. However, the effectiveness of the validation challenges confronted so far—mostly cases from steady state ion heated L-mode plasmas—is quite limited. Moreover, the validation domain of these exercises has been all *inside* familiar territory. Even then, results have not been satisfactory, in that the '$\rho > 0.6$ shortfall problem' has been faced in local gyro kinetic models [148], the leading transport model candidate. This problem might arguably be said to constitute a re-statement of the familiar 25+ year-old observation that local drift wave theories tend to fail as ρ increases, while the temperature drops. Non-locality phenomena are significant here, in that (i) they offer a novel road forward for resolving the shortfall issue, by core-edge coupling phenomena such as avalanching, spreading, etc., (ii) by their transient, multi-scale character, they constitute far more rigorous tests of transport models. In particular, the relation between fluctuations, transport and spatio-temporal dynamics over a wide range of space *and* time scale must be successfully predicted in order to declare victory in the modelling of such phenomena and (iii) they constitute a kind of 'terra nova' for validation studies—i.e., in this context, models can be forced to actually *predict* the outcome of *new* experiments, and cannot so easily be tuned to obtain a previously known 'right answer'. Points (i)–(iii) above all support the important role non-locality studies can and indeed *must* play in the world-wide programme of transport model validation for the development of magnetic fusion energy. Non-locality phenomena constitute the *central issue* and not some peripheral exotica, as claimed by some. We look forward to future contributions of model validation to non-locality studies with great interest.

Acknowledgments

We appreciate useful discussions at the Asian-Pacific Transport Working Group meetings. This work is partly supported by the Grant-in-Aid for Scientific Research of JSPS, Japan (21224014, 23244113, 23360414, 23246164, 23686134) and by the collaboration programmes of NIFS (NIFS10ULHH021, NIFS10KOAP023, NIFSULHH017) and of the RIAM of Kyushu University and Asada Science Foundation. This research was also supported by US Department of Energy (DOE) Contract No DE-FC02-99ER54512, the National Science Foundation of China under grant no

11261140326, R&D Programme through the National Fusion Research Institute of Korea (NFRI) funded by Government funds.

References

[1] Diamond P.H. *et al* 2010 *Modern Plasma Physics 1 Physical Kinetics of Turbulent Plasmas* (Cambridge: Cambridge University Press)
[2] Ida K. *et al* 1995 *Phys. Rev. Lett.* **74** 1990
[3] Gentle K.W. *et al* 1995 *Phys. Rev. Lett.* **74** 3620
[4] Mantica P. *et al* 1999 *Phys. Rev. Lett.* **82** 5048
[5] Inagaki S. *et al* 2006 *Plasma Phys. Control. Fusion* **48** A251
[6] Fujisawa A. *et al* 2009 *Nucl. Fusion* **49** 013001
[7] Diamond P. *et al* 2005 *Plasma Phys. Control. Fusion* **47** R35
[8] Hallatschek K. and Biskamp D. 2001 *Phys. Rev. Lett.* **86** 1223
[9] Nagashima Y. *et al* 2005 *Phys. Rev. Lett.* **95** 095002
[10] Drake J.F., Zeiler A. and Biskamp D. 1995 *Phys. Rev. Lett.* **75** 4222
[11] Diamond P. 2001 *Nucl. Fusion* **41** 1067
[12] Das A. Sen A. Mahajan S. and Kaw P. 2001 *Phys. Plasmas* **8** 5104
[13] Yamada T. *et al* 2008 *Nature Phys.* **4** 721
[14] Itoh S.-I. and Itoh K. 2011 *Plasma Phys. Control. Fusion* **53** 015008
[15] Inagaki S. *et al* 2011 *Phys. Rev. Lett.* **107** 115001
[16] Garbet X., Laurent L., Samain A. and Chinardet J. 1994 *Nucl. Fusion* **34** 963
[17] Wong K.L. *et al* 1999 *Plasma Phys. Control. Fusion* **41** R1
[18] Chen L. and Zonca F. 2007 *Nucl. Fusion* **47** S727
[19] Hahm T.S., Diamond P.H., Lin Z., Itoh K. and Itoh S.-I. 2004 *Plasma Phys. Control. Fusion* **46** A323
[20] Gürcan Ö.D. Diamond P.H., Hahm T.S. and Lin Z. 2005 *Phys. Plasmas* **12** 032303
[21] Garbet X. *et al* 2007 *Phys. Plasmas* **14** 122305
[22] Diamond P.H. and Hahm T.S. 1995 *Phys. Plasmas* **2** 3640
[23] Carreras B.A., Newman D., Lynch V.E. and Diamond P.H. 1996 *Phys. Plasmas* **3** 2903
[24] Newman D.E., Carreras B.A., Diamond P.H. and Hahm T.S. 1996 *Phys. Plasmas* **3** 1858
[25] Garbet X. and Waltz R.E. 1998 *Phys. Plasmas* **5** 2836
[26] Politzer P.A. 2000 *Phys. Rev. Lett.* **84** 1192
[27] Yoshizawa A., Itoh S-I. and Itoh K. 2002 *Plasma and Fluid Turbulence* (Bristol: Institute of Physics Publishing) chapter 25
[28] Ida K. *et al* 2008 *Phys. Rev. Lett.* **101** 055003
[29] Ida K. *et al* 2009 *Nucl. Fusion* **49** 015005
[30] Sun H.J. *et al* 2010 *Plasma Phys. Control. Fusion* **52** 045003
[31] Sun H.J. *et al* 2011 *Nucl. Fusion* **51** 113010
[32] Coppi B. 1980 *Comm. Plasma Phys. Control. Fusion* **5** 261
[33] Imbeaux F. *et al* 2001 *Plasma Phys. Control. Fusion* **43** 1503
[34] Garbet X. *et al* 2004 *Plasma Phys. Control. Fusion* **46** 1351
[35] Ida K. *et al* 2012 *Nucl. Fusion* **52** 027001
[36] Dong J.Q. *et al* 2013 *Nucl. Fusion* **53** 027001
[37] Jhang H. *et al* 2014 *Nucl. Fusion* **54** 047001
[38] Zaslavsky G.M. 2002 *Phys. Rep.* **371** 461
[39] Dif-Pradalier G. *et al* 2010 *Phys. Rev.* E **82** 25401
[40] Gürcan Ö.D. *et al* 2013 *Phys. Plasmas* **20** 022307
[41] Ida K. and Rice J. 2014 *Nucl. Fusion* **54** 045001
[42] Diamond P.H. *et al* 2009 *Nucl. Fusion* **49** 045002
[43] Diamond P.H. *et al* 2013 *Nucl. Fusion* **53** 104019
[44] Itoh S.-I. 1992 *Phys. Fluids* B **4** 796
[45] Sugama H. and Horton W. 1995 *Phys. Plasmas* **2** 2989
[46] Weiland J. 2000 *Collective Modes in Inhomogeneous Plasma* (Bristol: Institute of Physics Publishing)
[47] Diamond P.H. *et al* 2008 *Phys. Plasmas* **15** 012303
[48] Wang L. and Diamond P.H. 2013 *Phys. Rev. Lett.* **110** 265006
[49] Garbet X. *et al* 2013 *Phys. Plasmas* **20** 072502
[50] Inagaki S. *et al* 2013 *Nucl. Fusion* **53** 113006
[51] Nazikian R. *et al* 2005 *Phys. Rev. Lett.* **94** 135002
[52] Tamura N. *et al* 2005 *Phys. Plasmas* **12** 110705
[53] Tamura N. *et al* 2007 *Nucl. Fusion* **47** 449
[54] Ida K. *et al* 2006 *Phys. Rev. Lett.* **96** 125006
[55] Ida K. *et al* 2008 *J. Phys. Soc. Japan* **77** 124501
[56] Tamura N. *et al Proc. 23rd Int. Conf. on Fusion Energy 2010 (Daejeon, South Korea, 2010)* (Vienna:IAEA) CD-ROM file [EXC/P8-16] and www-naweb.iaea.org/napc/physics/FEC/FEC2010/index.htm
[57] Gürcan Ö.D. *et al* 2007 *Phys. Plasmas* **14** 042306
[58] Rice J. *et al* 2011 *Phys. Rev. Lett.* **106** 215001
[59] Ida K. *et al* 2010 *Nucl. Fusion* **50** 064007
[60] Rice J. *et al* 2013 *Nucl. Fusion* **53** 033004
[61] Rice J. *et al* 2011 *Phys. Rev. Lett.* **107** 265001
[62] Camenen Y. *et al* 2011 *Nucl. Fusion* **51** 073039
[63] Politzer P.A. *et al* 2002 *Phys. Plasmas* **9** 1962
[64] Xu Y.H. *et al* 2004 *Phys. Plasmas* **11** 5413
[65] van Milligen B.P. *et al* 2002 *Nucl. Fusion* **42** 787
[66] Stroth U. *et al* 2011 *Plasma Phys. Control. Fusion* **53** 024006
[67] Pedrosa M.A. *et al* 2008 *Phys. Rev. Lett.* **100** 215003
[68] Kadomtsev B.B. and Pogutse O.P. 1971 *Nucl. Fusion* **11** 67
[69] Itoh K. *et al* 2012 *Plasma Phys. Control. Fusion* **54** 095016
[70] Itoh S.-I. and Itoh K. 2001 *Plasma Phys. Control. Fusion* **43** 1055
[71] Inagaki S. *et al* 2012 *Nucl. Fusion* **52** 023022
[72] Tynan R.R., Fujisawa A. and McKee G. 2009 *Plasma Phys. Control. Fusion* **51** 113001
[73] Itoh S.-I. and Itoh K. 1988 *Phys. Rev. Lett.* **60** 2276
[74] Biglari H., Diamond P.H. and Terry P.W. 1990 *Phys. Fluids* B **2** 1
[75] Groebner R.J. *et al.* 1990 *Phys. Rev. Lett.* **64** 3015
[76] Ida K. *et al* 1990 *Phys. Rev. Lett.* **65** 1364
[77] Itoh S.-I. *et al* 1991 *Phys. Rev. Lett.* **67** 2485
[78] Kim E. *et al* 2003 *Phys. Rev. Lett.* **98** 185006
[79] Miki K. and Diamond P.H. 2012 *Phys. Plasmas* **19** 092306
[80] Conway G.D. *et al* 2011 *Phys. Rev. Lett.* **106** 065001
[81] Xu G.S. *et al* 2011 *Phys. Rev. Lett.* **107** 125001
[82] Schmitz L. *et al* 2012 *Phys. Rev. Lett.* **108** 155002
[83] Tynan G.R. *et al* 2013 *Nucl. Fusion* **53** 073053
[84] Cheng J. *et al* 2013 *Phys. Rev. Lett.* **110** 265002
[85] Estrada T. *et al* 2010 *Europhys. Lett.* **92** 35001
[86] Sugita S. *et al* 2012 *Plasma Phys. Control. Fusion* **54** 125001
[87] Sugita S. *et al* 2012 Transient response after change of input power intensity in edge turbulence *Int. Toki Conf. (Toki, Japan 2012)* P2-14 www.nifs.ac.jp/itc/itc22/
[88] Ghendrih Ph. *et al* 2012 Thermodynamical and microscopic properties of turbulent transport in the edge plasma *Proc. 25d Int. School of Plasma Physics on the Theory of Fusion Plasmas (Varenna, Italy, 2012)* http://varenna-lausanne.epfl.ch/Varenna2012/
[89] Itoh K., Itoh S.-I. and Fukuyama A. 1999 *Transport and Structural Formation in Plasmas* (Bristol: Institute of Physics Publishing) chapter 4
[90] Solomon W.M. *et al.* 2007 *Plasma Phys. Control. Fusion* **49** B313
[91] Sarazin Y. and Ghendrih Ph. 1998 *Phys. Plasmas* **5** 4214
[92] Beyer P., Benkadda S., Garbet X. and Diamond P.H. 2000 *Phys. Rev. Lett.* **85** 4892
[93] Idomura Y., Urano H., Aiba N. and Tokuda S. 2009 *Nucl. Fusion* **49** 065029
[94] Ku S., Chang C.S. and Diamond P.H. 2009 *Nucl. Fusion* **49** 115021
[95] Sarazin Y. *et al* 2010 *Nucl. Fusion* **50** 054004
[96] Iwasaki T., Itoh S.-I., Yagi M., Itoh K. and Stroth U. 1999 *J. Phys. Soc. Japan* **68** 478
[97] Iwasaki T., Itoh S.-I., Yagi M. and Itoh K. 2000 *J. Phys. Soc. Japan* **69** 722
[98] Sanchez R., van Milligen B.Ph. and Carreras B.A. 2005 *Phys. Plasmas* **12** 056105
[99] del-Castillo-Negrete D. 2006 *Phys. Plasmas* **13** 082308
[100] Calvo I., Garcia L., Carreras B.A., Sanchez R. and van Milligen B.Ph. 2008 *Phys. Plasmas* **15** 042302
[101] Ku S. *et al* 2012 *Nucl. Fusion* **52** 063013

[102] Abiteboul J. 2012 Transport turbulent et neoclassique de quantite de mouvement toroidale dans les plasmas de tokamak *PhD Thesis* Universite de Provence (Aix-Marseille), France
[103] Dif-Pradalier G. *et al* 2009 *Phys. Rev. Lett.* **103** 065002
[104] McMillan B.F., Hill P., Bottino A., Jolliet S., Vernay T. and Villard J. 2011 *Phys. Plasmas* **18** 112503
[105] Gorler T. *et al* 2011 *Phys. Plasmas* **18** 056103
[106] Bak P., Tang C. and Wiesenfeld K. 1988 *Phys. Rev.* A **38** 364
[107] Sanchez R., Newman D.E., Leboeuf J.-N., Decyk V.K. and Carreras B.A. 2008 *Phys. Rev. Lett.* **101** 205002
[108] Sarazin Y. *et al* 2012 Plasma size and collisionality scaling of ion temperature gradient driven turbulence *Proc. 24th IAEA Fusion Energy Conf. (San Diego, USA, 2012)* TH/P7-09 www-pub.iaea.org/iaeameetings/41985/24th-Fusion-Energy-Conference
[109] Nakata M. and Idomura Y. 2012 Plasma size and collisionality scaling of ion temperature gradient driven turbulence *Proc. 24th IAEA Fusion Energy Conf. (San Diego, USA, 2012)* TH/P7-07 www-pub.iaea.org/iaeameetings/41985/24th-Fusion-Energy-Conference
[110] Villard L. *et al* 2012 Global gyrokinetic ITG turbulence simulations of ITER *Proc. 25th Int. School of Plasma Physics on the Theory of Fusion Plasmas (Varenna, Italy, 2012)* http://varenna-lausanne.epfl.ch/Varenna2012
[111] Ghendrih Ph. *et al* 2005 *J. Nucl. Mater.* **337** 347
[112] McDevitt C.J., Diamond P.H., Gürcan Ö.D. and Hahm T.S. 2010 *Phys. Plasmas* **17** 112509
[113] Yi S., Diamond P.H., Kwon J.M. and Ku S. 2012 A new animal in the mesoscale zoo: Implications of non-resonant convective cells for turbulence intensity pro le, shear flow, and transport *Proc. 24th IAEA Fusion Energy Conf. (San Diego, USA, 2012)* PD/P8-19 www-pub.iaea.org/iaeameetings/41985/24th-Fusion-Energy-Conference
[114] Itoh K. *et al* 2009 *J. Plasma Fusion Res. Series* **8** 119
[115] Dritschel D.G. and McIntyre M.E. 2008 *J. Atmos. Sci.* **65** 855
[116] Rhines P.B. 1975 *J. Fluid Mech.* **69** 417
[117] Itoh K. and Itoh S.-I. 1996 *Plasma Phys. Control. Fusion* **38** 1
[118] Diamond P.H. 1995 *Phys. Plasmas* **2** 3685
[119] Kosuga Y., Diamond P.H. and Gürcan Ö.D. 2013 *Phys. Rev. Lett.* **110** 105002
[120] Van Milligen B.Ph., Sanchez R. and Carreras B.A. 2004 *Phys. Plasmas* **11** 2272
[121] Del-Castillo-Negrete D., Mantica P., Naulin V., Rasmussen J.J. and JET EFDA Contributors 2008 *Nucl. Fusion* **48** 075009
[122] Balescu R. 1995 *Phys. Rev.* E **51** 4807
[123] Zaslavsky G.M. 2005 *Hamiltonian Chaos and Fractional Dynamics* (Oxford: Oxford University Press)
[124] Malkov M.A. and Diamond P.H. 2008 *Phys. Plasmas* **15** 122301
[125] Taylor J.B., Connor J.W. and Helander P. 1998 *Phys. Plasmas* **5** 3065
[126] Kundu M., Deshpande S.P. and Kwap K. 2002 *Phys. Plasmas* **9** 3961
[127] Tendler M. 2010 *Plasma Fusion Res.* **5** S1004
[128] Itoh S.-I., Itoh K., Fukuyama A. and Yagi M. 1994 *Phys. Rev. Lett.* **72** 1200
[129] Kobayashi T. *et al* 2013 *Phys. Rev. Lett.* **111** 035002
[130] Tokuzawa T. *et al* 2014 *Phys. Plasmas* **21** 055904
[131] Shao L. 2013 private communication *3rd Asian-Pacific Transport Working Group Meeting (3rd APTWG) (Jeju Island, Korea, 2013)* http://aptwg2013.nfri.re.kr
[132] Han X. 2013 private communication *3rd Asian-Pacific Transport Working Group Meeting (3rd APTWG) (Jeju Island, Korea, 2013)* http://aptwg2013.nfri.re.kr
[133] Stroth U. *et al* 1996 *Plasma Phys. Control. Fusion* **38** 611
[134] Gentle K.W. *et al* 2006 *Phys. Plasmas* **13** 012311
[135] Itoh S-I. and Itoh K. 2012 *Sci. Rep.* **2** 860
[136] Itoh S.-I. and Itoh K. 2013 *Nucl. Fusion* **53** 073035
[137] Gürcan Ö.D. *et al* 2013 *Nucl. Fusion* **53** 073029
[138] Miki K. and Diamond P.H. 2010 *Phys. Plasmas* **17** 032309
[139] Itoh K., Itoh S.-I., Diamond P.H., Fujisawa A., Yagi M., Watari T., Nagashima Y. and Fukuyama A. 2006 *J. Plasma Fusion Res.* **1** 037
[140] Fu G.Y. 2008 *Phys. Rev. Lett.* **101** 185002
[141] Zarzoso D. *et al* 2013 *Phys. Rev. Lett.* **110** 125002
[142] Sasaki M., Itoh K. and Itoh S.-I. 2011 *Plasma Phys. Control. Fusion* **53** 085017
[143] Ido T. *et al* Observation of a new energy channel from energetic particles to bulk ions through geodesic acoustic mode *Proc. 24th IAEA Fusion Energy Conf. (San Diego, USA, 2012)* PD/P8-16 www-pub.iaea.org/iaeameetings/41985/24th-Fusion-Energy-Conference
[144] Hammett G.W. and Perkins F.W. 1990 *Phys. Rev. Lett.* **64** 3019
[145] Ida K. *et al* 2009 *Nucl. Fusion* **49** 095024
[146] Ida K. *et al* 2010 *Contrib. Plasma Phys.* **50** 558
[147] Kasuya N. *et al* Numerical Simulation of Plasma Turbulence and Diagnostics: Nonlinear Response to Source Modulation *7th Festival de Theorie (Aix-en-Provence, France, 2013)* www.festival-theorie.fr
[148] Holland C. *et al* 2009 *Phys. Plasmas* **16** 052301